THE REACTION CROSS SECTION OF NITROGEN 14 FOR PROTONS BETWEEN 220 KEV AND 600 KEV

Thesis by

Ralph Edward Pixley

In Partial Fulfillment of the Requirements

For the Degree of

Doctor of Philosophy

California Institute of Technology

Pasadena, California

1957

ACKNOWLEDGEMENT

I am indebted to the staff and to the graduate students of the Kellogg Radiation Laboratory for the assistance I have received in completing this research. In particular, I wish to thank Professors W. Whaling and W. A. Fowler. Professor Whaling has supervised this research and has assisted with the experiment. Discussions with Professor Fowler have been very helpful and stimulating.

I also wish to express my gratitude to Mr. Ehrgott who spent much time designing special equipment for this experiment and to Mr. Overly who assisted with operating and maintaining the equipment.

ABSTRACT

The yield of the reaction $N^{14}(p, \gamma)$ was measured between 220 and 650 kev using targets of beryllium nitride and tantalum nitride. The relative yield obtained by counting positrons was normalized to the absolute measurement at 285 kev of the annihilation radiation and prompt gamma-ray yields. Target composition was determined from elastic scattering measurements and from the yield of the $N^{14}(\alpha, p)O^{17}$ reaction. The cross section for the $N^{14}(p, \gamma)$ reaction was determined from 220 to 285 kev and from 400 to 600 kev. A resonance in the reaction was observed at 278.14 ± 0.4 kev with a width of 1.7 ± 0.5 kev.

The spectrum of prompt gamma rays was observed. The ratio of yield at 0 and 90 degrees was 1.00 ± 0.07 for the 0.75 Mev radiation and 0.97 ± 0.045 for the 1.34 Mev radiation. The 7.6 Mev radiation was less than 10 $^{o}/o$ of the 6.26 Mev radiation.

The cross section for $N^{14}(p, p)N^{14}$ was measured from 200 to 650 kev at 152 degrees. Measurements at 90, 125 and 152 degrees near the 278-kev resonance indicate that the 7.61 Mev state in O^{15} is $J = 1/2^{+}$.

Energy levels below 9 Mev in N^{15} and O^{15} are compared. It is found that one level near 7 Mev in N^{15} has not been detected in O^{15}. Extrapolation of the cross section to lower energies is uncertain due to this undetected level. The rate of the CN- cycle is discussed.

TABLE OF CONTENTS

ILLUSTRATIONS

I. INTRODUCTION

Energy generation in stars resulting from the conversion of hydrogen into helium by a series of nuclear reactions occurs in several distinct ways, the two most important being the direct proton-proton chain and the carbon-nitrogen cycle. Previous measurements of the cross sections for the reactions in the CN- cycle indicate that the reaction of nitrogen 14 with protons has the smallest cross section at the proton energies found in stars (1). The rate of this reaction thus limits the rate of energy production by the CN- cycle and it is of interest to measure the reaction cross section as accurately as possible.

The cross section for this reaction is too small to be measured in the laboratory at the proton energies to be found in stars. It is necessary to extrapolate from measurements made at higher energies. The extrapolation is guided by the properties of levels in the compound nucleus and involves the Coulomb penetration factor.

The present work was originally undertaken to measure the cross section in the energy range between 128 kev and 600 kev and thus connect the measurements of Woodbury, Hall and Fowler (2) at 128 kev with the measurements of Duncan and Perry (3) above 278 kev. However, the cross section proved to be smaller than that predicted by the 128 kev measurement, and it was impossible to measure the cross section below 220 kev with the proton current available from the 650 kev electrostatic generator. The measurement of the cross section is described in Section II.

The only reaction energetically possible in this energy range other than the elastic scattering is gamma-ray emission:

$$N^{15} + p \rightarrow O^{15*} \rightarrow O^{15} + \gamma \qquad Q = 7.347 \text{ Mev} \qquad (1.1)$$

The ground state of the residual nucleus decays by positron emission:

$$O^{15} \rightarrow N^{15} + \beta^{+} + \nu \qquad Q = 2.705 \text{ Mev} \qquad (1.2)$$

It is possible to measure the cross section by detecting the prompt gamma rays, the positrons or the annihilation radiation. It was convenient to use each of these three methods of detection in different phases of the present experiment, the choice being determined by consideration of background, counter efficiency and accuracy.

A resonance occurs in the reaction cross section at 278 kev proton energy (4). In order to determine the spin and parity of the state in O^{15} corresponding to this resonance, the cross section for elastic scattering of protons from nitrogen 14 was measured. The spin and parity of the state as determined from this measurement was inconsistent with a previous measurement of the angular distribution of prompt gamma rays. The angular distribution of the prompt gamma rays was remeasured and found to be consistent with the elastic scattering experiment. The elastic scattering measurement is described in Section III and the angular distribution of prompt gamma rays is described in Section II-5-D.

The spectrum of prompt gamma rays was determined in order to measure the yield and angular distribution of the prompt gamma rays. The excitation function for prompt gamma rays was measured from 275 kev to 330 kev in order to determine the width of the 278 kev resonance. This measurement of the width was used to distinguish between the assignments, $J = 3/2^{+}$ and $J = 1/2^{+}$, as determined in the elastic scattering experiment. The gamma-ray measurements are described in Section II-5.

Section IV discusses the energy levels of O^{15} and the extrapolation of the measured cross section to 25 kev.

II. REACTION CROSS SECTION

General Procedure

The reaction cross section is determined by measuring the yield of the reaction as a function of energy. The yield of a reaction for a given incident particle energy is defined as the number of reactions occurring per incident particle for a specified target. The yield determined by counting the prompt gamma rays from the $N^{14}(p, \gamma)$ reaction is simply

$$Y = \frac{e\,N}{Q\,\mathrm{eff}} \tag{2.1}$$

where

Y is the yield for a specified target at energy E

Q is the charge collected on the target in coulombs

e is the electron charge in coulombs

N is the number of reactions detected

eff is the efficiency of the gamma detector.

The yield determined by counting the delayed positrons or annihilation radiation is measured in a slightly different way. One method is to bombard the target with a constant proton current for a specified time and then to count positrons or annihilation radiation for a definite counting period with no beam on the target. The yield in this case is

$$Y = \frac{e\,N}{i_\infty \tau\ \mathrm{eff}\ (e^{-t_1/\tau} - e^{-t_2/\tau})} \tag{2.2}$$

where

Y is the yield for a specified target at energy E

N is the number of positrons or 1/2 the number of annihilation quanta detected

eff is the efficiency of the detector

e is the electron charge in coulombs

$i_\infty = i_o(1 - e^{-t_o/\tau})$

i_o is the constant proton current in amperes

τ is the mean life of the decaying nucleus in seconds

t_o is the bombarding time in seconds

$t_2 - t_1$ is the counting period in seconds beginning at time t_1 after the beam is turned off.

The factor, i_∞, is the equivalent constant current which produces the same activity for an infinite bombarding time as i_o produces in the bombarding time, t_o. A method of current integration will be described in Section II-B which determines i_∞ for a proton current that is not constant.

The yield expressed in terms of the reaction cross section is

$$Y = \int_0^{\Delta x} \sigma(x)\, n\, dx = \int_{E_1 - \Delta E}^{E_1} \frac{\sigma(E)}{\epsilon(E)}\, dE \qquad (2.3)$$

where

σ is the reaction cross section in cm^2

n is the number of target nuclei for the reaction per cm^3

Δx is the target thickness in cm

ΔE is the target thickness in kev

ϵ is the stopping cross section per nitrogen atom in the tar-

get expressed in kev-cm^2

E_1 is the incident proton energy in kev.

A thick target is one that stops the incident proton. The cross section in terms of a thick target yield is

$$\sigma(E) = \epsilon(E) \frac{dY}{dE} \qquad (2.4)$$

where

σ is the reaction cross section in cm^2

ϵ is the stopping cross section per nitrogen atom of the target expressed in kev-cm^2

Y is the thick target yield measured at the energy E.

A thin target is one in which σ and ϵ change very little in the energy thickness of the target. The cross section in this case is given by

$$\sigma(E) = \frac{\epsilon Y}{\Delta E} \qquad (2.5)$$

where

σ is the reaction cross section in cm^2 at the energy E

ϵ is the stopping cross section per nitrogen atom of the target expressed in kev-cm^2

Y is the thin target yield measured at the energy E_1

ΔE is the target thickness in kev

$E \approx E_1 - \frac{1}{2}\Delta E$ all expressed in kev.

Since a yield can be measured for a target containing nitrogen along with other elements, it is convenient for comparison purposes to determine the equivalent yield for a target of the same thickness containing only nitrogen. For the approximation that ϵ/ϵ_N is constant in the energy

thickness of the target producing most of the yield, the equivalent nitrogen target yield, Y_N, in terms of the measured yield, Y, is

$$Y_N = \frac{\epsilon}{\epsilon_N} Y \qquad (2.6)$$

where

ϵ is the stopping cross section of the target per atom of nitrogen expressed in kev-cm^2

ϵ_N is the stopping cross section per nitrogen atom expressed in kev-cm^2.

In the present work this approximation was more accurate than the experimentally measured stopping cross sections. Throughout the remainder of this thesis we shall refer only to the yield of a nitrogen target although this yield was actually determined from a target containing a nitrogen compound.

The following different measurements were used in this experiment to determine the yield: 1) Absolute thick target yield at 285 kev bycounting annihilation radiation; 2) absolute thick target yield from 270 to 330 kev by counting prompt gamma radiation; 3) relative thick target yield from 218 to 400 kev by counting positrons and 4) relative thin target yield from 400 to 600 kev by counting positrons. The annihilation radiation and prompt gamma-ray measurements could be made only for thick targets above the 278 kev resonance since the reaction counting rate at other energies was much less than the background counting rate. The efficiency of the positron counter was much greater than the gamma counter efficiency and the background was much lower permitting thick target yield measurements appreciably below the 278 kev resonance and thin target

measurements above 400 kev; however, the continuous spectrum of the positrons and the back scattering from the target made absolute measurements very difficult. All positron yield measurements were normalized by comparison with the absolute yield measurements at 285 kev.

Equipment

The equipment used in this experiment was primarily that associated with the 650 kev electrostatic generator of the Kellogg Radiation Laboratory. Much of this equipment is of standard design and will only be briefly mentioned in this thesis.

The 650 kev electrostatic generator and its operation have been described by Wenzel (6). For the present experiment the ion source was changed to an RF source of the type described by Moak (7). Only the H^+ beam was used in this experiment. Proton currents up to 100 microamperes were obtained from this source.

The energy of the protons was determined and stabilized by an electrostatic analyzer (8). A magnetic field was used to separate the various mass components before the beam reached the analyzer. Proton currents up to 50 microamperes were available at the target.

A double focussing, magnetic analyzer was completed and tested during the latter part of this experiment. It was used only in the measurement of the gamma-ray angular distribution. Proton currents of 90 microamperes were obtained at the target.

The double focussing magnetic spectrometer used in the elastic scattering measurement is shown in fig. 1. This spectrometer, which

is very similar to the one described by Snyder, Rubin, Fowler and Lauritsen (9), deflects charged particles through 165 degrees. The solid angle of the spectrometer is 0.006 steradians. The momentum resolution, $P/\Delta P$, can be varied from 50 to 600.

TARGET CHAMBER. The target chamber used in the positron yield measurements is shown schematically in fig. 2. The target could be rotated from a vertical position in the proton beam to a horizontal position near the thin CsI(Tl) crystal used to detect the positrons. A similar arrangement was used to measure the yield of annihilation radiation. The CsI(Tl) crystal was replaced by a lucite plate to stop the positrons and a NaI(Tl) crystal was used to detect the annihilation radiation.

Standard techniques were used to insure that the charge measured on the target was due to only the incident protons. A tantalum aperture trimmed the proton beam to 3/16 of an inch in diameter. A guard ring, held at minus 300 volts, was located between this aperture and the target chamber. The target chamber including the target was held at a positive 300 volts. The guard ring thus prevented electrons scattered from the beam trimming aperture from reaching the target and also prevented secondary electrons from leaving the target.

ANNIHILATION RADIATION DETECTOR. A NaI(Tl) crystal, 1.5 inches long by 1.5 inches in diameter, was used to detect the annihilation radiation. The crystal was mounted on a Dumont type 6292 photomultiplier. The crystal was separated from the activated target in its counting position by a 1/2 inch thick lucite plate. The positrons were stopped by

this lucite plate and by the target backing in a small volume near the target surface.

The pulse height spectrum was recorded on a ten channel pulse height discriminator. A typical spectrum for annihilation radiation is shown in fig. 3. The background increases for lower pulse heights; therefore, only the photo peak of the annihilation spectrum was used to measure the yield.

The photo peak efficiency of the counter is the number of pulses recorded in the photo peak of the spectrum divided by the number of annihilation quanta. This efficiency for annihilation radiation was measured directly by the coincidence method using a Na^{22} source and an auxiliary counter. Sodium 22 decays 90 $^{o}/o$ of the time by positron emission to the 1.28 Mev state in Ne^{22}, 10 $^{o}/o$ by K capture to the same state and less than 1 $^{o}/o$ by positron emission directly to the ground state (10) of Ne^{22}. The 1.28 Mev state emits a single gamma ray to the ground state. Therefore, for every one hundred 1.28 Mev gamma rays, one expects 90 positrons or 180 annihilation quanta. The Na^{22} source was placed in the same position occupied by the target after bombardment. A tantalum backing was used to stop the positrons. The auxiliary counter was placed nearby and biased to count only the 1.28 Mev radiation. The auxiliary counter was used to gate the ten channel analyzer which recorded the spectrum of pulses obtained from the main counter. The photo peak efficiency of the main counter was therefore the number of counts in the photo peak divided by 1.8 times the number of gate pulses. This method of measuring efficiency takes into account the absorption of the radiation in the lucite between the target and the counter.

The relative probable error in the measured photo peak efficiency is due to 1), change in photomultiplier and amplifier gain during the measurement and 2), the statistical uncertainty of the photo peak counts. For this experiment, all of the spectrum above the minimum just below the photo peak was used for the photo peak. See fig. 2. The spectrum of the photo peak covered 8 channels on the pulse height analyzer. A change in gain resulting in a 1/2 channel spectrum shift would affect the number of counts in these 8 channels by only 5 °/o. A larger change in gain would have been corrected. The counting statistics were 3 °/o. Thus the relative probable error in the photo peak efficiency is 6 °/o. The measured photo peak efficiency was 0.0265 $\pm$ 0.001 for a positron source located 0.52 inches from the counter and with a 1/2 inch thick sheet of lucite between the source and counter.

As a check on the efficiency measurement, the total efficiency for annihilation radiation was computed using the linear absorption coefficient of NaI (11). The ratio of the number of counts in the photo peak to the total number of counts in the spectrum was measured. See fig. 2. The photo peak efficiency determined in this way was 0.025 $\pm$ 0.0025. The accuracy of this number is somewhat uncertain. The linear absorption coefficient was obtained from a curve which could be read to 5 °/o accuracy. The uncertainty in the measured ratio of photo peak to total spectrum is approximately 10 °/o due to counting statistics and extrapolation of the spectrum to zero energy.

EFFICIENCY OF PROMPT GAMMA DETECTOR. The same 1.5 x 1.5 inch NaI crystal located 1.5 inches from the target was used to measure the absolute yield from the prompt gamma rays. Analysis of the prompt gamma-ray spectrum (see Section II-5-A) shows that the efficiency of

the counter must be known for 0.75, 1.34 and 2.4 Mev gamma rays. Due to the complex spectrum it is convenient to use the photo peak efficiency. The total efficiency for gamma rays of each of these energies was computed using the linear absorbtion coefficient of NaI (11). The ratio of photo peak to total efficiency was measured for the 0.661 Mev radiation of Cs^{137}, the 1.28 Mev radiation of Na^{22} and the 2.61 Mev radiation of Th C". The ratios at the required energies, 0.75, 1.34 and 2.4 Mev, were obtained by interpolation.

The photo peak efficiencies obtained in this way are 0.0049 ± 0.0006 for the 0.75 Mev radiation, 0.0022 ± 0.003 for the 1.34 Mev radiation and 0.0009 ± 0.0002 for the 2.4 Mev radiation. The relative probable error is slightly larger for the 2.4 Mev radiation since the pair plus one peak increases the uncertainty in the photo peak.

POSITRON DETECTOR. The positron detector used in this experiment was a thin crystal of Cs(Tl), 1/2 inch in diameter and 0.02 of an inch thick. A Dumont type 6291 photomultiplier was used. The target after bombardment was 0.005 of an inch from the front surface of the crystal resulting in a counter solid angle of almost 2π. The maximum energy positrons from O^{15} have an energy of 1.733 Mev (12). A crystal 0.02 of an inch thick does not stop the higher energy positrons that enter perpendicular to the surface. Thus the pulse height spectrum is not a true representation of the energy spectrum of the positrons. Every positron entering the crystal gives a pulse proportional to its energy loss in the crystal. The very thin crystal was used to minimize the cosmic ray background. Since the cosmic ray background increased rapidly for lower pulse heights, the pulse height dis-

criminator was set to accept pulses corresponding to positrons losing at least 400 kev in the crystal. The cosmic ray background for this bias setting was 2.5 counts per minute.

CURRENT INTEGRATOR. A modification was incorporated in the beam current integrator which permitted i_∞ (see equation 2.2) to be determined without maintaining a constant beam current. The method used was to allow the collected charge to leak off the integrator capacitor with an exponential decay constant just equal to the mean life of O^{15}. The voltage on the integrator capacitor at any time was then proportional to the activity initiated in the target by the beam. The exponential decay constant of the integrator was created by placing a resistor in parallel with the integrator capacitor such that $RC = \tau$.

The yield in terms of the integrator components can be determined by comparing the differential equation for the O^{15} build-up with the equation for the electrical circuit.

$$\frac{dn}{dt} = \frac{Y}{e}\frac{dq}{dt} - \frac{n}{\tau} \qquad (2.7)$$

$$\frac{dV}{dt} = \frac{1}{C}\frac{dq}{dt} - \frac{V}{RC} \qquad (2.8)$$

where

n is the number of O^{15} nuclei present at any time t

t is the time in seconds after the beam is turned on

τ is the mean life of O^{15} in seconds

Y is the yield of the reaction per proton

q is the charge collected on the target in coulombs

e is the electron charge in coulombs

V is the integrator voltage at time t

C is the integrator capacitor in farads

R is the parallel resistor such that $RC = \tau$.

Equation 2.8 is identical to equation 2.7 with the substitution $V = en/YC$. The yield is then given by

$$Y = en/VC = enR/V\tau \tag{2.9}$$

The integrator is set to turn the beam off at a specified voltage, V_o. Comparison of equation 2.9 with $V = V_o$ and equation 2.2 shows that

$$i_\infty = V_o/R \tag{2.10}$$

The relative probable error in i_∞ as determined by this method of integration depends on the uncertainty of V_o, R and τ , the equality $RC = \tau$, and the magnitude of the current. For the case of constant current, i_∞ is given accurately by

$$i_\infty = \frac{V_o}{R} \frac{(1 - e^{-t_o/\tau})}{(1 - e^{-t_o/RC})} \tag{2.11}$$

For this case the relative probable error in using $i_\infty = V/R$ is

$$RPE = \left\{\left(\frac{\delta V_o}{V_o}\right)^2 + \left(\frac{\delta R}{R}\right)^2 + \left[\frac{e^{-t_o/\tau}}{(1-e^{-t_o/\tau})} \frac{t_o}{\tau}\right]^2 \left[\left(\frac{\delta \tau}{\tau}\right)^2 + \left(\frac{RC - \tau}{\tau}\right)^2\right]\right\}^{1/2} \tag{2.12}$$

where RPE stand for the relative probable error and δ refers to the uncertainty in the various quantities. The factor $\frac{e^{-t_o/\tau}}{1-e^{-t_o/\tau}} \frac{t_o}{\tau}$ of the third

term of equation 2.12 has its maximum value of 1 when $t_o = 0$. In the present experiment the uncertainty of V_o is 2 °/o, R is 1 °/o, and RC is equal to τ within 2 °/o. The maximum value of the relative probable error for i_∞ computed from equation 2.12 is 3 °/o. The accuracy of this integrator was checked experimentally by making runs at the same energy with different beam currents. The initial counting rate in each case was within a few percent of the same value indicating proper operation of the integrator.

Target Preparation and Analysis

There are only a few target materials containing nitrogen that will withstand the beam current necessary for this experiment. The protons lose all of their energy in a very thin layer at the front of the target and the heat produced must be conducted away fast enough to prevent the target's decomposition. An ideal target would be stable at high temperature and would be a good heat conductor. No nitrogen compound was found to be a good heat conductor thus making it necessary to keep the actual target very thin and use a high conductivity target backing. One method of doing this is to nitride a surface layer of certain metals.

Two types of targets used in this experiment were made by nitriding beryllium and tantalum. The nitride layer was of the order of 50 kev thick for 300 kev protons which corresponds to approximately 10^{-5} of an inch. The targets were prepared by heating the metal in ammonia at a pressure of approximately 0.1 atmosphere. Sheet tantalum was available that could be heated by electric current in the bell jar. The available beryllium was of such dimensions that it had to be heated in a quartz tube

with a Bunsen burner. The metal was first heated to a bright orange heat to outgas. Ammonia which had passed through a cold trap at approximately -50 degrees Centigrade to remove the water was admitted to the system. The metal was heated to an orange heat for several minutes. The heating is rather critical for beryllium as too high a temperature for too long a time causes the nitride to flake off. The beryllium was heated several times at progressively higher temperatures until the nitride formed a gray surface on the metal. It was necessary to outgas the system very thoroughly for the beryllium to prevent oxide formation. The tantalum heating was not critical and no trouble was experienced with the formation of the oxide. The tantalum nitride targets made in this way are blue.

The tantalum nitride targets were very easy to make and were used wherever possible in the experiment. The tantalum targets were unsatisfactory for the thin target measurements above the resonance as the nitrogen tended to straggle deep into the target and did not form a well defined layer. The beryllium nitride targets formed a better layer with less straggling and were used for the thin target measurements.

Although both types of target were used to measure the absolute thick target yield below the resonance and at a single energy just above the 278 kev resonance, they were unsatisfactory to measure the variation in the thick target yield with energy above the resonance. The concentration of nitrogen varied too rapidly with depth in the target. A sintered titanium nitride target used in the Woodbury, Hall and Fowler experiment (2) was used to measure the variation in thick target yield above the resonance.

TARGET ANALYSIS. In order to find the cross section per nitrogen atom, it is necessary to know the stopping cross section of the target per nitrogen atom. See Section II-1. This was measured by elastic scattering of 1.65 Mev protons for the beryllium nitride target and by the $N^{14}(\alpha, p)O^{17}$ reaction at the 3.1 Mev resonance for the tantalum nitride target. The stopping cross section of the target per nitrogen atom as measured using a spectrometer to analyze the scattered or reaction particles is

$$\epsilon_1 = \frac{2q\Omega}{eR} \frac{E_2 \frac{d\sigma}{d\Omega}}{(\alpha + \eta + E_{10} \frac{\partial \alpha}{\partial E_{10}}) N} \qquad (2.13)$$

where the subscript 1 refers to the incident particle, the subscript 2 refers to the reaction particle, the subscript 10 refers to the incident particle just before the reaction and the subscript 20 refers to the reaction particle just after the reaction

ϵ is the stopping cross section per nitrogen atom in kev-cm^2

E is the energy in kev

φ is the angle between the particle direction and the target normal

q is the charge collected on the target in coulombs

e is the electron charge in coulombs

Ω is the center of mass solid angle of the spectrometer

R is the spectrometer momentum resolution, $P/\Delta P$

$\frac{d\sigma}{d\Omega}$ is the differential cross section

N is the number of particles counted

$$\eta = (\epsilon_2/\epsilon_1)(\cos\varphi_1/\cos\varphi_2)$$

$$\alpha = \frac{E_{20}}{E_{10}} = \left\{ \frac{M_1M_2}{M_2+M_3} \left\{ 2\cos^2\theta + \frac{M_o(M_2+M_3)}{M_1M_2} \left[\frac{Q}{E_{10}} + 1 - \frac{M_1}{M_o} \right] \right\} \right.$$
$$\left. \pm 2\cos\theta \left\{ \cos^2\theta + \frac{M_o(M_2+M_3)}{M_1M_2} \left[\frac{Q}{E_{10}} + 1 - \frac{M_1}{M_o} \right] \right\}^{1/2} \right\}$$

θ is the spectrometer angle.

The value of ϵ_1 is actually determined for some energy between E_1 and E_{10} such that $\epsilon_1 = (E_1 - E_{10}) / \int_{E_{10}}^{E_1} \frac{dE}{\epsilon_1}$. Similarly, ϵ_2 is for an energy between E_{20} and E_2 such that $\epsilon_2 = (E_{20} - E_2) / \int_{E_2}^{E_{20}} \frac{dE}{\epsilon_2}$. The partial derivative, $\frac{\partial \alpha}{\partial E_{10}}$, is zero for the elastic scattering but is important for the (α, p) reaction. The derivative of η with respect to E_{10} has been taken to be zero which is a good approximation for both reactions at the energies used in the measurements.

Protons of 1.65 Mev were used for the beryllium nitride analysis rather than protons of several hundred kev in order to separate the protons scattered from the layers of O^{16} and N^{14}. The momentum profile is shown in fig. 4. The value of the $N^{14}(p, p)N^{14}$ cross section was measured by Webb, Hagedorn, Mozer and Fowler (13). It is useful to determine also the stopping cross section per atom of oxygen and per atom of beryllium in the target. Using the scattering cross sections measured by Laubenstein and Laubenstein (14) for oxygen and the cross section for beryllium measured by Mozer (15), the composition of the target is found to be $Be_3N_{1.7}O_{0.4}$, which differs little from the known chemical compound, beryllium nitride, Be_3N_2. This measured compo-

sition represents the greatest nitrogen concentration which occurs at the front surface of the target. Several points on the target were checked and found to have the same maximum concentration of nitrogen.

The relative probable error in the peak value of ϵ_1 at 278 kev as determined by the measurement at 1.65 Mev is 11 %. The individual uncertainties are shown in Table I.

TABLE I

Source of error	Relative probable error in source	Relative probable error in ϵ_1 (278 kev)
$\frac{d\sigma}{d\Omega}(N^{14})$	8 %	4 %
$\frac{d\sigma}{d\Omega}(Be^{9})$	10	7
$\frac{d\sigma}{d\Omega}(O^{16})$	10	1
ϵ(Be) 1.65 Mev	3	2
ϵ(N) 1.65 Mev	5	2
ϵ(O) 1.65 Mev	5	<1
$\frac{\epsilon'}{\epsilon}$ Be $\frac{0.28 \text{ Mev}}{1.65 \text{ Mev}}$	5	2
$\frac{\epsilon'}{\epsilon}$ N "	3	2
$\frac{\epsilon'}{\epsilon}$ O "	5	<1
$q\Omega/R$	5	5
$\frac{\partial \eta}{\partial E}_{10} = 0$	1	1
N for N^{14}	4	2
N for Be^{9}	1	1
N for O^{16}	5	1
α	<1	<1
E_2	<1	<1
		RMS total = 11 %

The reaction $N^{14}(\alpha, p)O^{17}$ was used to analyze the composition of the tantalum nitride targets. The cross section for this reaction at 90 degrees center of mass angle and at the peak of the 3.1 Mev resonance has been measured by Heydenburg and Temmer (16) to be 5.2×10^{-27} cm^2 and more recently by Herring et al. (17) to be $(6.1 \pm 0.1) \times 10^{-27}$ cm^2. The Q value of the reaction is -1.198 Mev and the resonance is 120 kev wide. The 16 inch magnetic spectrometer with resolution width much less than the width of either the target or the resonance was used to determine the spectrum of protons produced in the reaction. The scattered alpha particles were stopped by a 0.00025 of an inch thick aluminum foil. Momentum profiles of the protons were obtained for different bombarding energies near the resonance energy. The highest peak counting rate which was obtained when the resonance energy occurred at the target layer of maximum nitrogen concentration was used in equation 2.13 to determine ϵ_1 for 3.1 Mev alpha particles in the target. From this value the target composition was determined to be $Ta_{0.94}N$. This assumes the target to be only tantalum and nitrogen and uses the approximate relation that the stopping cross section of alpha particles is four times the stopping cross section for protons of the same velocity. There are two known nitrides of tantalum, TaN and Ta_3N_5. The target analyzed in this experiment is almost completely TaN. The value of ϵ_1 at 278 kev for the peak nitrogen concentration of the target as computed from the target composition determined in this experiment has a relative probable error of 14 %. The individual uncertainties of this measurement are shown in Table II.

TABLE II

Source of error	Relative probable error in source	Relative probable error in ϵ_1 (278 kev)
$\frac{d\sigma}{d\Omega}$	5 %	5 %
$\frac{q\Omega}{R}$	5	5
ϵ_α (1.65 Mev), N	≈10	5
ϵ_α (1.65 Mev), Ta	≈10	5
$\frac{\epsilon'}{\epsilon}$, N, $\frac{0.278 \text{ Mev protons}}{1.65 \text{ Mev } \alpha}$	≈10	5
$\frac{\epsilon'}{\epsilon}$, Ta, "	≈10	5
$\frac{\partial \alpha}{\partial E}_{10}$	1	< 1
N	5	5
α	< 1	< 1
E_2	< 1	< 1
$\frac{\partial \eta}{\partial E}_{10} = 0$	< 1	< 1
		RMS total = 14 %

Annihilation Radiation Yield

The absolute thick target yield measured by counting annihilation quanta was determined at 285 kev for both a tantalum nitride and a beryllium nitride target. A typical run will be described. The target was bombarded with 285 kev protons until the integrator reached 100 volts at which time the beam was automatically turned off. This integrator voltage corresponded to an i_∞ of 22.2 microamperes (see section II-2-F). The target was then rotated nearer the counter, as shown in fig. 1. The counter was turned on twenty seconds after the beam was turned off. Five 2-1/2 minute counting periods were used on

each run to observe the 2 minute half-life of the O^{15} decay. One minute counter off periods were required between each of the 2-1/2 minute counting periods to record the data. The ten channel pulse height discriminator was used to analyze the photo peak spectrum of the annihilation radiation absorbed in the 1.5 x 1.5 inch NaI(Tl) crystal (see Section II-2-C).

The yield per proton at 285 kev for a thick nitrogen target was computed from equations 2.2 and 2.6. Only the first counting period of each run was used to determine the yield as the statistical accuracy of the measurement decreased with longer counting periods. The average of two runs on each target was used to determine the yield. The uncertainty in the number of photo peak counts on each run was 6 °/o; 3 °/o was due to counting statistics of the reaction counts plus background and 5 °/o was allowed for possible shift of the pulse height spectrum (see Section II-2-C).

The error in the timing of the counting period was 1 second for t_1 and 1 second for t_2 (see equation 2.2). The relative probable error in the yield due to the uncertainty in t_1 and t_2 is found to be 0.6 °/o. The mean life, τ, was measured to 1 °/o accuracy. The relative probable error in the yield due to the uncertainty in τ is 0.3 °/o.

The absolute yield determined at 285 kev was measured for a target with nonuniform nitrogen concentration. This yield is expected to be only slightly less than the yield at 285 kev for a uniform target with the same nitrogen concentration as the front surface of the nonuniform target. The difference is expected to be small since the O^{15} is made by protons in a very small energy range near 278 kev.

The effect of the nonuniform nitrogen concentration was estimated in the following way. A method for finding the approximate stopping cross section per nitrogen atom of the target as a function of depth in the target using the yield measured above 278 kev is described in the appendix. The ratio of the yield at 285 kev for the nonuniform and the uniform target can then be found by substituting this stopping cross section in equation 2.3 and numerically integrating the result. The reaction cross section was taken to have the form of the single level resonance formula with $\Gamma = 1.7$ kev. The value of the ratio of yields for the nonuniform and uniform targets was found to be 0.93 ± 0.04 for both the beryllium nitride and tantalum nitride targets.

Table III shows the individual errors in the yield determination. The thick nitrogen target yield over the entire resonance was found to be $(1.62 \pm 0.23) \times 10^{-11}$ betas per proton for the beryllium nitride measurement and $(2.18 \pm 0.36) \times 10^{-11}$ for the tantalum nitride measurement. The weighted mean is 1.78×10^{-11} betas per proton. The internal error computed from the probable error of each measurement is 0.19×10^{-11}. The external error computed from the two measured yields is 0.16×10^{-11}. This indicates that the accuracy of the two measurements is consistant with the assigned errors.

Previous measurements of this yield are somewhat higher than this value. Duncan and Perry (3) obtain 3.5×10^{-11} betas per proton. Bashkin, Carlson and Nelson (5) obtain $(2.2 \pm 0.5) \times 10^{-11}$ by measuring the positrons and $(2.7 \pm 0.5) \times 10^{-11}$ from a measurement of the prompt gamma radiation.

The reason for the discrepancy is unknown. The yields obtained from two different targets analyzed by independent methods give one con-

fidence in the determination of the target composition in the present experiment. As a check on the counting equipment, the $C^{12}(p, \gamma)$ yield was measured using a solid graphite target. The reaction is very similar to the $N^{14}(p, \gamma)$ reaction and the yield has been accurately determined. Using the same techniques of the $N^{14}(p, \gamma)$ measurement the yield measured at 600 kev for the $C^{12}(p, \gamma)$ reaction was in good agreement with the measurement by Seagrave (18).

The effect of O^{15} escaping from the target was determined to be small by a measurement of the prompt gamma-ray yield described in the next section.

TABLE III

RELATIVE PROBABLE ERROR IN THE ABSOLUTE YIELD MEASUREMENT

Source of Error	Error	Error in the Berylium Nitride Measurement	Error in the Tantalum Nitride Measurement
$\frac{\epsilon(Be_3N_2)}{\epsilon(N)}$	10 %	10 %	----
$\frac{\epsilon(TaN)}{\epsilon(N)}$	14		14 %
Correction for target uniformity	4	4	4
i_∞	3	3	3
Number of counts	4	4	4
Timing	1	1	1
Mean life	1	1	1

Relative probable error in the beryllium nitride measurement = 14 %

Relative probable error in the tantalum nitride measurement = 17 %

Prompt Gamma-Ray Measurements

SPECTRUM. A 4 inch long by 4 inch diameter NaI(Tl) crystal located 1.5 inches from the target was used to study the gamma rays above 3 Mev. The pulse height spectrum obtained with this crystal is shown in fig. 5. A 1.5 inch long by 1.5 inch diameter NaI(Tl) located 1.5 inches from the target was used to measure the gamma-rays spectrum from 0.65 Mev to 3 Mev. This spectrum is shown in fig. 6. It was not possible to measure the spectrum below 0.65 Mev due to the large background of annihilation radiation.

The low energy spectrum shows well defined gamma rays at 0.755 ± 0.03 Mev and 1.34 ± 0.05 Mev. There is also a weaker gamma ray at 2.40 ± 0.10 Mev. The energy scale of the pulse height spectrum was calibrated by using the natural gamma-ray sources, Cs^{137} at 0.661 Mev, Na^{22} at 1.28 Mev and Th C" at 2.62 Mev. The energies determined for the three low energy gamma rays are in good agreement with similar measurements made by Johnson, Robinson and Moak (19) and by Bashkin, Carlson and Nelson (5). A summary of these gamma-ray energy determinations is given in Table IV.

The high energy spectrum although not as well resolved shows three gamma rays at approximately 6.8, 6.3 and 5.2 Mev. The pairs of gamma rays at 6.8 and 0.755 Mev, 6.3 and 1.34 Mev and at 5.2 and 2.40 Mev are in cascade.

There are also a few pulses corresponding to 7.6 Mev radiation; however, most of these are due to capture in the crystal of both cascade quanta. This was determined by observing the ratio of 7.6 Mev to 6.3 Mev pulses as the counter was moved farther from the source. The apparent 7.6 Mev radiation decreased more rapidly than the 6.3 Mev radi-

ation. An upper limit to the actual 7.6 Mev radiation was determined to be 10 °/o of the 6.3 Mev radiation. Johnson et al. (19) observe no 7.6 Mev radiation. Bashkin et al. (5) place an upper limit on the 7.6 Mev radiation of 5 °/o of the 6.3 Mev radiation.

TABLE IV

GAMMA-RAY ENERGIES

Johnson, et al.	Bashkin, et al.	Present Experiment
0.75 ± 0.03 Mev		0.755 ± 0.03 Mev
1.39 ± 0.03		1.34 ± 0.05
2.38 ± 0.10		2.40 ± 0.10
5.29 ± 0.10	5.25 ± 0.10 Mev	5.2
6.21 ± 0.10	6.10 ± 0.10	6.26
6.84 ± 0.10	6.65 ± 0.15	6.85

PROMPT GAMMA-RAY YIELD. The three low energy gamma rays were used to determine the total yield at 285 kev from the same tantalum nitride target that was used in the annihilation yield measurement. The efficiency of the counter for each of the three gamma rays was determined from the linear absorbtion coefficient of NaI as described in Section II-2-D. The total yield of these three gamma rays for a thick nitrogen target over the entire 278 kev resonance was found to be $(1.8 \pm 0.4) \times 10^{-11}$ per proton. Table V shows the individual source of error of this measurement. For purposes of comparing the prompt gamma-ray measurement with the annihilation measurement, the error associated with the stopping cross sections and the target uniformity should not be included, as the same target was used for both measurements. The

ratio of the yield obtained by the prompt gamma-ray measurement to the annihilation radiation measurement is 0.83 ± 0.18. This result implies that the escape of O^{15} from the target is small since any loss of O^{15} during bombardment and counting would cause this ratio to be greater than 1.

TABLE V

RELATIVE PROBABLE ERROR IN PROMPT GAMMA-RAY YIELD

Source of Error		Error	Error in yield
eff	0.75 Mev	15 %	4
	1.34	15	9
	2.4	20	3
Counts	0.75	25	6
	1.34	10	6
	2.40	50	8
Integrator		5	5
$\frac{\epsilon(TaN)}{\epsilon(N)}$		14	14

Relative probable error in yield = 22 %

EXCITATION FUNCTION. The thick target excitation function of prompt gamma rays was measured to determine the energy and width of the resonance near 278 kev. The measurement of the prompt gamma-ray excitation function required much less time than the positron or annihilation radiation measurement thereby reducing errors due to drift

of equipment. This prompt gamma-ray excitation function was also used to determine the thick target yield from 271 kev to 335 kev relative to the absolute measurement at 285 kev. The target contained a small amount of F^{19} contaminant which produced a large background of 6 Mev radiation for proton energies near the 340 kev resonance in $F^{19}(p, \alpha, \gamma)O^{16}$ thus preventing measurement of the excitation function above 335 kev. The target also contained N^{15} which produced a large yield of 4.4 Mev radiation near 430 kev from the resonance in $N^{15}(p, \alpha, \gamma)C^{12}$.

The resonance energy was determined from the energy of the half-maximum point of the excitation function shown in fig. 7. The electrostatic analyzer was calibrated by the 2.9 kev wide resonance in $F^{19}(p, \alpha, \gamma)O^{16}$ at 340.4 ± 0.4 kev (20). The energy measured for the nitrogen resonance was 278.14 ± 0.53 kev. The probable error is due to the following uncertainties: the fluorine resonance energy, 0.4 kev; determination of the midpoints of the excitation curves for nitrogen and fluorine, 0.2 kev each and possible surface layers on the targets, 0.2 kev.

The width of an isolated narrow resonance can be determined from the thick target excitation function. The width, Γ, of the resonance at half maximum is the difference in energy between the 3/4 maximum yield and 1/4 maximum yield points (21). This difference was found to be 2.0 ± 0.4 kev for the 278 kev resonance but must be corrected for finite resolution. The resolution window of the electrostatic analyzer is approximately 0.5 kev and the target voltage varies 0.1 kev. The correction for the energy window reduces the resonance width to 1.9 kev for a Gaussian window shape or 1.95 kev for a square window shape. The lower limit of the measured width was decreased by an additional 0.1 kev

to allow for surface effects. Thus the resonance width determined from this measurement is $1.9^{+0.4}_{-0.5}$ kev.

The only previous measurement of the width and energy of this resonance was made by Tangen (4). He reports the resonance energy to be 277 $\pm$ 2 kev and the width to be less than 2 kev. He also reports the fluorine resonance to be at 339 $\pm$ 2 kev indicating that his absolute energy scale may be 1 kev low in this energy range.

ANGULAR DISTRIBUTION OF PROMPT GAMMA RAYS. The ratio of yield at 0 and 90 degrees was measured for the 0.755 Mev and the 1.34 Mev gamma rays. The front surface of the 1.5 x 1.5 inch NaI(Tl) crystal was located 1.5 inches from the target. The crystal, photo multiplier and preamplifier were mounted on an arm which pivoted about the axis of a cylindrical target chamber 2-1/2 inches in diameter. The target chamber was made of lucite with walls 1/4 inch thick.

A sintered titanium nitride target was bombarded at 300 kev with a proton current between 70 and 90 microamperes. The beam spot was 1/8 inch in diameter. The distance from the center of the beam spot to the front of the crystal was the same at 0 and 90 degrees to within 0.005 inch. The target was positioned at 45 degrees with respect to the beam so that the gamma rays passed through the same amount of target material to reach the detector at 0 and 90 degrees.

The pulse height spectrum obtained at 0 and 90 degrees is shown in fig. 8. The channel width of the pulse height discriminator corresponds to 25 kev of the spectrum. Each point represents the average of two runs of 0.015 coulombs each. In order to average out any drift in the pulse height spectrum, runs were alternated between 0 and 90 degrees (four

runs for the same setting of the ten channel discriminator).

The shaded area of the spectrum between 0.9 Mev and 1.45 Mev in fig. 8 was used to determine the ratio of the yield at 0 and 90 degrees for the 1.34 Mev gamma ray. Only the photo peak counts were used for the 0.755 Mev determination. The ratio of the number of counts attributed to the 1.34 Mev gamma ray at 0 and 90 degrees was found to be 0.97 ± 0.045. The ratio for the 0.755 Mev gamma ray was 1.00 ± 0.07. The relative probable error in these ratios due to counting statistics was determined from the expression

$$RPE = \frac{0.67\sqrt{2}\sqrt{N_T + N_{BG} + N_{CR} + (\delta N_{BG})^2 + (\delta N_{CR})^2}}{N_T - N_{BG} - N_{CR}} \qquad (2.14)$$

where

N_T is the total number of counts at either angle due to a single gamma ray and the background

N_{BG} is the background due to higher energy gamma rays

N_{CR} is the background due to cosmic rays

δN_{BG} and δN_{CR} are the uncertainties in the backgrounds.

Since the pulse height spectrum between 0.6 Mev and 1.5 Mev shows no evidence for gamma rays other than the 0.755 and 1.34 Mev radiation, the background due to higher energy gamma rays was determined from the spectrum immediately above the gamma ray being measured. Although the spectrum of this background may not be exactly flat, the shape of this spectrum should be the same at both angles and thus the shape of the background spectrum will affect the ratio, N(0)/N(90), only slightly. The ratio of the background at 0 and 90 degrees due to higher energy gamma rays was 1.00 ± 0.07 for the 1.34 Mev gamma ray ($\sqrt{2}\,\frac{\delta N_{BG}}{N_{BG}} = 0.07$)

and 1.00 ± 0.06 for the 0.755 Mev gamma ray ($\sqrt{2}\,\frac{\delta N_{BG}}{N_{BG}} = 0.06$).

The isotropy of these gamma rays determined in this experiment is consistent with the assignment of $1/2^+$ for the state in O^{15} at 7.61 Mev, as determined from the elastic scattering experiment described in Section III.

Positron Yield Measurements

The thick target yield was measured from 218 kev to 300 kev by counting positrons. Targets similar to the tantalum nitride target described in Section II-3 were used for this measurement. The detector and target chamber are described in Sections II-2-E and II-2-B.

The procedure followed in this experiment was very similar to that of the annihilation radiation measurements. The target was bombarded until the integrator reached 100 volts, at which point the beam was automatically turned off. This integrator voltage corresponded to $i_\infty = 22.2$ microamperes. The target was then moved nearer the counter. The counter was turned on 20 seconds after the beam was turned off. The counter was biased to count positrons that lost more than approximately 400 kev in the CsI(Tl) crystal.

For high counting rates, 30 second counting periods were used with 30 seconds between each counting period to record the data. For low counting rates, the total number of counts was read from the scalers every 30 seconds (no counter off time). The counting rate for each run was observed until it had decayed to almost the background level (20 to 30 minutes).

This long counting period was used to determine the initial counting

rate due to only the O^{15}. Below the 278 kev resonance the counting rate of positrons from N^{13} formed in the C^{12} + p reaction became troublesome. The N^{13} half life is 10 minutes. The background due to the N^{13} could be determined by observing the counting rate after the O^{15} counting rate had died out. The C^{12} in the target increased with continued bombardment. Below 250 kev, targets were replaced after four runs which represented a total charge of approximately 20,000 microcoulombs.

At 218 kev, the lowest energy for which the yield was measured, the initial O^{15} counting rate was approximately equal to the background counting rate of 2-1/2 counts per minute. Hall (22) has determined that the counting period which minimizes the statistical uncertainty of a reaction counting rate between 1 and 10 times background is between 2 and 3.5 half lives. Therefore, the number of counts obtained during the first 5 minutes (2.5 half lives) was used to determine the initial counting rate for each run.

The initial counting rate at each energy was compared to the counting rate at 285 kev. Every fifth run was made at 285 kev to check that the target had not deteriorated and that the counting efficiency had not changed. Variations in the initial counting rate obtained at 285 kev were less than 10 %.

In fig. 9 the initial counting rate is plotted versus energy and the point at 285 kev is normalized to the absolute yield determined for this energy. This curve represents the thick target yield as a function of energy. A small correction has been made for the nonuniform target composition as discussed in the Appendix.

The same experimental procedure was used for the thin target yield measurements. A beryllium nitride target was used as the layer

containing nitrogen was more sharply defined than in the tantalum nitride targets. The yield of this target below 330 kev was essentially a thick target yield. The initial counting rate at 285 kev was normalized to the absolute yield determined for this energy. The target thickness was determined from the apparent width of the 278 kev resonance. The target was found to be approximately 50 kev thick at 328 kev. The yield curve in fig. 10 thus represents the yield of a nitrogen target 50 kev thick and is a thin target yield above 450 kev. The measurements between 330 kev and 450 kev are not meaningful in terms of either a thick target yield or a thin target yield. The yield from the resonance is decreasing rapidly in this region due to the rapid decrease of nitrogen concentration with depth in the target.

Table VI lists the relative probable error in the yield of a thick nitrogen target determined at energies between 220 and 285 kev. The relative probable error in the absolute normalization at 285 kev is 15 °/o as determined in Section II-4. The error in integration is discussed in Section II-2-F and is 3 °/o. The error in timing the counting period is less than 1 °/o. The relative probable error in the number of counts due to the O^{15} decay was computed from the expression

$$\frac{\delta N_1}{N_1} = \frac{0.67\sqrt{N + N_o + N_2 + \left(\frac{\delta C_o}{C_o} N_o\right)^2 + \left(\frac{\delta C_2}{C_2} N_2\right)^2}}{N - N_o - N_2} \qquad (2.15)$$

where

N is the total number of counts obtained in the counting period

N_1 is the number of counts due to O^{15}

N_2 is the number of counts due to N^{13}

N_o is the number of cosmic ray background counts

C_o is the cosmic ray counting rate

C_2 is the initial N^{13} counting rate

δC_o and δC_2 are the uncertainties in these rates.

The background due to N^{13} was determined for each run by observing the counting rate after the O^{15} counting rate had died out.

The effect of the nonuniform target composition on the yield is expected to be small since the cross section decreases very rapidly for the lower energies and therefore most of the yield is obtained from the front surface of the target. The ratio of the nonuniform target yield to the uniform target yield, Y/Y_o, was computed at 220 kev and 250 kev using the value of $\frac{\epsilon}{\epsilon_o}(\Delta x)$ determined in Section II-4. The effect on Y/Y_o of the resonant and nonresonant yield was computed separately. Using the form of the cross section given in equation 4.9, the value of Y/Y_o at 220 kev was found to be 0.89 due to the resonant part of the cross section and 0.81 for the nonresonant part. At 250 kev, the resonant part of Y/Y_o is 0.90 and the nonresonant is 0.76. The average Y/Y_o for the resonant and nonresonant yield weighted according to their relative contribution to the total yield is 0.84 ± 0.10 at 220 kev and 0.89 ± 0.07 at 250 kev.

The same type of uncertainties occurring for the thick target yield measurement also occur for the thin target yield measurement. The effect of the nonuniform target is slightly different. The ratio of the nonuniform target yield, Y, to the yield, Y_1, of a target of finite thickness which has the same composition as the front surface of the nonuniform target was computed. The ratio of the yield Y/Y_1 is found to be 1.00 ± 0.10 at 550 kev for a uniform target which is 50 kev thick for 328 kev protons. The value 1 is merely a result of the arbitrary choice

TABLE VI

ACCURACY OF THE THICK TARGET YIELD

Proton Energy (kev)	Uncertainty in N	Uncertainty in Y
220	50 %	52 %
230	14	19
240	11	17
250	9	15
260	5	13
270	3	12
280	2	11

TABLE VII

ACCURACY OF THE THIN TARGET YIELD

Proton Energy (kev)	Uncertainty in N	Uncertainty in Y
450	7 %	14 %
500	6	13
550	4	13
600	3	12
650	2	12

of the comparison target thickness. The relative probable error in the yield between 450 kev and 600 kev for a nitrogen target 50 kev thick at 328 kev is listed in Table VII.

Cross Section

The cross section was determined from the thick target and thin target yields using equations 2.4 and 2.5. Between 276 and 284 kev the thick target yield was graphically differentiated. Below 276 kev it was convenient to differentiate $\log_{10} Y$ rather than Y. The value of dY/dE is then

$$dY/dE = (\log_{10} e)\, Y\, d \log Y/dE \qquad (2.16)$$

Between 220 and 250 kev the value of d log Y/dE is nearly constant. The value of d log Y/dE is much more accurately known than Y. Therefore, the relative error in the value of dY/dE was approximated by the relative error in the yield. Between 250 kev and 276 kev the value of d log Y/dE is increasing rapidly and the relative probable error of d log Y/dE is comparable to the error in N. As an approximation in this energy range, the relative probable error in dY/dE was taken to be the sum of the relative probable error in Y and N. From 276 to 284 kev the yield was graphically differentiated to approximately 10 $^{o}/_{o}$ accuracy. The error in the cross section due to the uncertainty in ϵ has been included in the error determined for the yield. The error in the cross section is shown as brackets for representative points in fig. 11.

The cross section could not be measured with meaningful accuracy between 284 and 450 kev. The relative change in the thick target yield

with energy above the resonance was too small to be accurately determined. The nitrogen in the thin targets was not in a well defined layer but tended to straggle deep into the target, thus preventing thin target yield measurements in this layer.

The relative probable error in the cross section determined from the thin target yield is equal to the relative probable error in this yield. The error in cross section due to ϵ and to ΔE of equation 2.5 has been included in the error determined for Y.

ELASTIC SCATTERING

Cross Section Measurements

The cross section for elastic scattering of protons from nitrogen has been studied by several observers (13), (23), (24); however, previous measurements do not extend below 620 kev. Of special interest is the energy region near 278 kev where capture cross section work has shown a resonance which is approximately 2 kev wide.

A thick target suitable for elastic scattering measurements of protons from N^{14} must contain no element heavier than nitrogen; the stopping cross section must be known; it must have a smooth surface; and it must be stable under proton bombardment. The target material used in this experiment was the organic compound, melamine. Its chemical composition is $(N_2CH_2)_3$. The target was prepared in vacuum by evaporating a thick layer of melamine on an aluminum backing.

The counting rate versus incident proton energy, with the spectrometer field held constant, is shown in figs. 12 and 13. It is seen from these two energy profiles that the number of protons scattered from only the nitrogen in the target can be easily determined at scattering angles greater than or equal to 85.9 degrees. These profiles also show that there are no elements heavier than nitrogen in the target. The peaking of the C^{12} step in fig. 12 shows the effect of carbon build-up on the front surface of the target with continued bombardment. A new target spot produced the step without the carbon peak.

The cross section for elastically scattered protons is given by the expression (9)

$$\frac{d\sigma}{d\Omega}(E_{10}) = 2 \frac{e}{Q} \frac{R}{\Omega} \frac{N}{E_2} \left[\bar{\epsilon}_1 \frac{E_{20}}{E_{10}} + \bar{\epsilon}_2 \frac{\cos\varphi_1}{\cos\varphi_2} \right] \qquad (3.1)$$

where

$\frac{d\sigma}{d\Omega}$ is the differential cross section in cm^2 per steradian at the energy E_{10} and the scattering angle θ

E_1 is the analyzer energy, expressed in kev

E_{10} is the energy of the incident proton just before it is scattered, expressed in kev

E_{20} is the energy of the scattered proton just after it is scattered, expressed in kev

E_2 is the spectrometer energy, expressed in kev

$\frac{Q}{e}$ is the number of incident protons

R is the momentum resolution of the spectrometer, $P/\Delta P$

Ω is the center of mass solid angle of the spectrometer

$\bar{\epsilon}_1$ is the stopping cross section per nitrogen atom at an energy between E_1 and E_{10} such that

$$\bar{\epsilon}_1 = (E_1 - E_{10}) \Big/ \int_{E_{10}}^{E_1} \frac{dE}{\epsilon}$$

$\bar{\epsilon}_2$ is the stopping cross section per nitrogen atom at an energy between E_{20} and E_2 such that

$$\bar{\epsilon}_2 = (E_{20} - E_2) \Big/ \int_{E_2}^{E_{20}} \frac{dE}{\epsilon}$$

both stopping cross sections expressed in kev-cm^2

N is the number of counts

φ_1 is the supplement of the angle made by the target normal

and the incident beam

φ_2 is the angle between target normal and spectrometer.

The reaction energy is given by (9)

$$E_{10} = \left(E_2 + \frac{\bar{\epsilon}_2 \cos\varphi_1}{\bar{\epsilon}_1 \cos\varphi_2} E_1\right) / \left(\frac{E_{20}}{E_{10}} + \frac{\bar{\epsilon}_2 \cos\varphi_1}{\bar{\epsilon}_1 \cos\varphi_2}\right) \qquad (3.2)$$

The constant $2eR/Q\Omega$ was determined by scattering from copper which is known to be Rutherford (25) except for a small correction due to electron shielding. The shielding correction has been worked out by Wenzel (26). The cross section for copper is

$$\frac{d\sigma}{d\Omega}(Cu) = \frac{d\sigma}{d\Omega}(\text{Rutherford}) \left[1 - \frac{3.65}{E_{10}}\right] \qquad (3.3)$$

where E_{10} is expressed in kev.

The stopping cross section for melamine, $(N_2CH_2)_3$, has not been measured directly; however, C_2H_4 and N_2 have been measured by Reynolds, Dunbar, Wenzel and Whaling (27). They observe Bragg's law to be accurate above 200 kev so that the stopping cross section of melamine per nitrogen atom is given by 1/4 the stopping cross section of C_2H_4 plus 1/2 the stopping cross section of N_2.

At lower energies an increasing percentage of the scattered protons pick up an electron in leaving the target. Electron capture by protons is dependent on the composition of the surface layer of the target; however, the neutral fraction is negligible above 300 kev and still small at 200 kev for all materials (28). The correction to the cross section used in this experiment was 2 ^{o}/o at 250 kev and 4 ^{o}/o at 200 kev corresponding to a target surface composed of diffusion pump oil.

The absolute cross section was measured at a center of mass scattering angle of 152 degrees from 200 to 650 kev. The ratio of the measured cross section to Rutherford is shown in fig. 14. The relative probable error in the absolute cross section is 7 °/o made up of the following individual uncertainties: stopping cross section of N_2, C_2H_4 and Cu, 3 °/o each; counting statistics, 2 °/o; reproducibility of the integrator, 1 °/o; effect of uncertainty in spectrometer and target angles, 1 °/o each and spectrometer energy, 1/2 °/o. The counting rate was observed to decrease with continued bombardment of the same target spot. Therefore, each target spot was used for only two runs of 10 microcoulombs each. The correction for this bombardment was 1 °/o on the first run and 3 °/o on the second.

The cross section at the center of mass scattering angle of 152 degrees is within 5 °/o of Rutherford from 200 to 350 kev except for the narrow resonance at 278 kev. At higher energies the cross section rises, reaching 1.17 times Rutherford at 650 kev. This is in good agreement with the value, 1.21 times Rutherford, obtained by Hagedorn, Mozer, Webb, Fowler and Lauritsen (13), at 650 kev for a center of mass scattering angle of 154 degrees.

Spin and Parity of the 7.61 Mev State

The angular momentum, ℓ , of the incident protons forming a narrow resonance can be determined by measuring the scattering cross section at angles corresponding to the zeroes of Legendre polynomials. Mozer (29) has shown that the interference term in the theoretical expression for the scattering amplitude of a narrow resonance with at most an s-

wave and Coulomb background has the angular dependence of $P_\ell^o(\cos\theta)$ where ℓ is the orbital angular momentum of the incident protons forming the state. Thus there is no interference minimum in the scattering cross section at angles corresponding to the zeroes of $P_\ell^o(\cos\theta)$.

Near the 278 kev resonance, the scattering cross section was measured at three angles, 90, 125 and 152 degrees in the center of mass. The ratio of the scattering cross section to Rutherford is shown in figs. 15, 16 and 17. Interference minima occur at all three angles. The 90 degree minimum rules out formation of the level by odd ℓ-value protons as 90 degrees is the zero of Legendre polynomials of odd ℓ. Formation by d-wave protons is ruled out by the minimum at 125 degrees, the zero of $P_2^o(\cos\theta)$. Higher ℓ values can be excluded on the basis that the measured width would then exceed the single particle limit. (The measured width is discussed in Section II-5-C.) Thus, only s-wave formation is possible.

The spin and parity of N^{14} is known to be 1^+, and the spin of the proton is 1/2 so that the spin and parity of the state in O^{15} at 7.61 Mev formed by s-wave protons is either $1/2^+$ or $3/2^+$. The size of the anomaly in the scattering cross section at the resonance is determined by the spin of the level. The theoretical expression for the scattering cross section of s-wave protons at a narrow resonance with a background of s-wave and Coulomb scattering as worked out by Mozer (29) simplifies to the following equation in the case of no reaction cross section other than gamma-ray emission.

$$\frac{\sigma(\theta)}{\sigma_R} - 1 = \frac{2J+1}{6} \left\{ \begin{array}{l} \left(-\frac{2}{k\sqrt{\sigma_R}} \cos \xi\right) \sin(\delta+\varphi) \cos(\delta+\varphi) \\ +\left(\frac{1}{k^2 \sigma_R} + \frac{2}{k\sqrt{\sigma_R}} \sin \xi\right) \sin^2(\delta+\varphi) \end{array} \right\} \quad (3.4)$$

where

$\sigma(\theta)$ is the differential scattering cross section

σ_R is the differential Rutherford cross section

J is the spin of the state

k is the wave number given by $\frac{\sqrt{2\mu E_{cm}}}{\hbar}$

u is the reduced mass

E_{cm} is the center of mass energy of the reaction

ξ is the Coulomb phase shift given by $\xi = \frac{Ze^2\mu}{\hbar^2 k} \ln \sin^2 \frac{\theta}{2}$

δ is the resonance parameter given by $-\delta = \text{arc cot} \frac{E-E_R}{\frac{1}{2}\Gamma}$

Γ is the half width of the resonance

E_R is the resonance energy

θ is the scattering angle

φ is the nonresonant phase shift.

The nonresonant s-wave phase shift is expected to be small at 278 kev. An upper limit for it can be obtained from the absolute value of the off-resonance cross section. The absolute cross section is Rutherford within a 10 ^{o}/o uncertainty at 250 and 300 kev. This uncertainty corresponds to a possible nonresonant phase shift of 8 degrees. A zero degree phase shift was used to compute the theoretical curves in fig. 15, 16 and 17; however, an 8 degree phase shift alters these curves only slightly.

It is seen that the anomaly for a J = 3/2 resonance is twice as large as a J = 1/2 resonance; however, the measured anomaly is never quite as large as the theoretical one due to the resolution of the measuring equipment. The apparent width of the 278 kev anomaly is about as large as the 2 kev computed resolution. The measured size of the anomaly is approximately 70 °/o of the J = 1/2 theoretical value or 35 °/o of the J = 3/2 value. On the basis of just this elastic scattering data it is impossible to distinguish between a J = 1/2 level with a width approximately equal to the resolution and a J = 3/2 level with a width of about one quarter the resolution. However, the width of this resonance has also been measured in the (p, γ) reaction. This measurement described in Section II-5-C was made with 1/2 kev resolution and shows the resonance to be $1.9 \pm \begin{matrix} 0.4 \\ 0.5 \end{matrix}$ kev wide. The elastic scattering measurement is then to be interpreted as J = $1/2^+$ level of width 1.5 ± 0.5 kev. The experimental cross section at 152, 125 and 90 degrees center of mass is shown in figs. 14, 15 and 16 along with the theoretical curves for a J = $1/2^+$ level 1.5 kev wide.

The assignment, J = $1/2^+$, is in disagreement with the measurement of the prompt gamma-ray angular distribution made by Bashkin, Carlson and Nelson (5). They obtain the ratio of the yield of the 6.2 and 5.2 Mev gamma rays at 0 and 90 degrees to be 1.07 ± 0.03. Their measurement indicates that the state could not be formed by s-wave protons; however, the elastic scattering experiment is much more conclusive than the 7 °/o deviation in the very difficult gamma-ray measurement. The angular distribution of the 0.755 and 1.34 Mev gamma rays was found to be isotropic in Section II-5-D of the present experiment.

IV. EXTRAPOLATION OF THE CROSS SECTION

Energy Levels of N^{15} and O^{15}

A resonance in the N^{14} + p reaction occurring below 100 kev could have a very large effect on the rate of the CN-cycle and yet not be noticed in the measured yield above 200 kev. Other types of experiments must be used to discover any levels in this critical energy range. Reactions which lead to the same compound or residual nucleus yield additional information about states in this energy range. Another method of locating states in this region involves using information about corresponding states in the mirror nucleus, N^{15}. The states of N^{15} are well determined from the N^{14}(d, p) reaction (30), (31).

Of the various reaction which yield direct information about states in O^{15}, only the N^{14}(d, n)O^{15} reaction has been examined carefully in the energy range of interest. The results are inconclusive. The d, n stripping reaction was measured by Evans, Green and Middleton (32) for 7.7 Mev deuterons using nuclear emulsions to detect the neutrons and determine their energy. The statistical accuracy and energy resolution of this experiment were insufficient to detect a weak group corresponding to a level near 7.4 Mev. The N^{14}(d, n)O^{15} neutron threshold measurement of Marion, Bruggers and Bonner (33) was also inconclusive in this energy range due to the large background of neutrons to the 6.8 and 6.91 Mev levels which obscured any weak thresholds at higher energy.

The energy levels of O^{15} and N^{15} are shown in fig. 18. Dotted lines are drawn joining corresponding levels of the two nuclei. This pairing of corresponding levels was determined on the basis of level shift calcu-

lations and the measured spin and parity of the states.

The difference in energy of corresponding levels in mirror nuclei due to 1, nuclear boundary conditions, 2, spin-orbit interaction and 3, nuclear volume expansion with excitation has been discussed by Thomas (34). He computes the level shift to be the order of 50 kev due to 2 and 3 for corresponding levels near 3 Mev in N^{13} and C^{13}. Larger level shift differences are due to 1. The effect of 1 is of the order of 1 Mev for levels with large reduced widths. Accurate data for computing the small effect due to 2 and 3 are not available for O^{15} and N^{15}. The level shift referred to in the remainder of this thesis is that due to the boundary conditions only.

The level shifts were computed from formulae derived by Thomas (34). Only the level shift due to the proton width was considered for the levels in O^{15} and only the shift due to the neutron width was considered for the levels in N^{15}. The level shift is then given by

$$\Delta_c = -\gamma^2 g_c^{Re} \qquad (4.1)$$

where

Δ_c is the level shift in Mev for the level c

γ^2 is the reduced width of this level in Mev-cm

g_c^{Re} is the real part of the logarithmic derivative of F evaluated at the nuclear surface

F is the solution of the external wave equation for outgoing waves.

The quantity of interest, $\Delta_n - \Delta_p$, is the difference between the level shifts for the corresponding levels in each nucleus. This difference is

just equal to the difference between the energy of the corresponding states in N^{15} and O^{15}, assuming the ground states to have no level shift.

For bound levels in O^{15}, the value of the reduced width, γ^2, is unknown. The procedure used for these levels was to assume the Wigner sum-rule limit for the reduced width and thereby compute the maximum possible level shift. This maximum possible value is useful when it is less than the level spacing as it is for the 5.2 Mev and 6.26 Mev levels in O^{15}. The reduced widths for the 7.6 Mev and 8.32 Mev levels of O^{15} were computed from the measured proton widths using the penetration factor calculated by Christy and Latter (35). The reduced width, γ^2, is given by

$$\frac{\gamma^2}{a} = \frac{\Gamma_p}{2P_\ell} ka \qquad (4.2)$$

where

$$a = (1.41 \times 10^{-13} \text{ cm})(\sqrt[3]{14} + 1) = 4.8. \times 10^{-13} \text{ cm}$$

$$ka = \frac{E_{cm}}{E_R}$$

E_{cm} is the center of mass proton energy

$$E_R = \frac{\hbar^2}{2\mu a^2} = 0.97 \text{ Mev}$$

u is the reduced mass = 14/15 a.m.u.

P_ℓ is the penetration factor for angular momentum ℓ

Γ_p is the measured proton width

The Wigner sum-rule limit, γ^2_{max}, is given by

$$\frac{\gamma^2_{max}}{a} = 3E_R \qquad (4.3)$$

The value of g_c^{Re} for the bound levels in O^{15} and the corresponding

levels in N^{15} was computed from the WKB approximation (34)

$$ag_c^{Re} = -\xi + \frac{(\ell + 1/2)^2 + \frac{E_c}{2E_R}}{2\xi^2} \qquad (4.4)$$

where

$$\xi = \left[(\ell + 1/2)^2 + \frac{E_c}{E_R} - \frac{E_{cm}}{E_R}\right]^{1/2}$$

$E_c = e^2/a = 2.1$ Mev for O^{15}

$E_{cm} = E_o - Q$

E_o = energy of the state above the ground state in Mev

Q = binding energy of a proton in O^{15} or a neutron in N^{15}

(7.347 Mev and 10.83 Mev respectively)

$E_R = \hbar^2/2\mu a^2 = 0.97$ Mev

ℓ is the angular momentum of the proton or neutron

From elastic scattering measurements (23), the 8.33 Mev level of O^{15} is found to be $3/2^+$. Thus both the 7.6 Mev and 8.33 Mev levels are formed by s-wave protons. The value of $\Delta\lambda_p$ for the 7.6 Mev and 8.33 Mev states of O^{15} was computed from the exact expression for g_c^{Re} for s-wave protons

$$g_c^{Re} = \left[F_o \frac{\partial F_o}{\partial r} + G_o \frac{\partial G_o}{\partial r}\right] / \left[F_o^2 + G_o^2\right] \qquad (4.5)$$

where G_o and F_o are the Coulomb wave functions tabulated by Bloch et al. (36). The level shift for the level in N^{15} corresponding to the 7.6 Mev and 8.33 Mev levels in O^{15} were computed from the exact expression for states formed by s-wave neutrons:

$$ag_c^{Re} = -ka \qquad (4.6)$$

The maximum possible level shift, $\Delta\lambda_p - \Delta\lambda_n$, determined for the 5.28 and 5.31 Mev levels in N^{15} is -0.75 Mev. This value was obtained using the Wigner sum-rule limit for the reduced width and for s-wave neutrons. It is slightly less for higher angular momentum neutrons. The corresponding levels must lie between 5.31 Mev and 4.53 Mev in O^{15}. Only one level in O^{15} has been reported in this region. It is at 5.2 Mev. Either this reported level represents two unresolved levels in O^{15} or else another level exists in O^{15} between 4.53 Mev and 5.31 Mev.

The level at 6.33 Mev in N^{15} has a maximum possible level shift, $\Delta\lambda_p - \Delta\lambda_n$, of -0.6 Mev. This value was obtained using the Wigner sum-rule limit for the reduced width and p-wave neutrons. The stripping reaction indicates that the level is $J \leq 5/2^-$. There is only one level between 5.73 and 6.33 Mev in O^{15}. It is at 6.26 Mev. The $N^{14}(d, n)$ stripping reaction indicates that this state is $J \leq 5/2^-$.

The maximum possible level shifts for higher energy levels is not useful as the level shift, $\Delta\lambda_p - \Delta\lambda_n$, is considerably greater than the level spacing; however, the level shift for the 7.6 Mev and 8.33 Mev levels of O^{15} formed by s-wave protons (13), can be computed using the measured widths in O^{15}. The level shift, $\Delta\lambda_p - \Delta\lambda_n$, is found to be 0.62 Mev and 0.007 Mev for the 7.6 Mev and 8.33 Mev levels respectively. This predicts the corresponding levels in N^{15} to be at 8.22 and 8.34 Mev. The only levels found between 7.58 and 9.06 Mev in N^{15} are at 8.32 Mev and 8.57 Mev. The $N^{14}(d, n)$ stripping reaction shows these two levels to be $1/2^+$ or $3/2^+$. The stripping reaction also shows the higher energy level to have a much smaller reduced width. Thus the 7.6 Mev

level of O^{15} corresponds to the 8.32 Mev level of N^{15} and the 8.33 Mev level of O^{15} corresponds to the 8.57 Mev level of N^{15}. It is apparent that there is an additional level shift of the order of 200 kev in this region of excitation which is not accounted for by the nuclear boundary conditions.

Between 6.33 and 8.32 Mev there are three levels in N^{15} and between 6.26 and 7.6 Mev, the corresponding range in O^{15}, there are only two reported levels. The 7.32 Mev level of N^{15} and the 6.85 Mev level of O^{15} are believed to be corresponding levels on the basis of similar stripping results. It is not possible to say whether it is the 7.58 Mev or the 7.16 Mev level in N^{15} that corresponds to the 6.91 Mev level of O^{15}, but in either case, there is one undetected level in O^{15} near 7 Mev.

The extrapolation of the measured cross section to 25 kev is very much uncertain due to this undetected level. The level in O^{15} corresponding to the 7.58 Mev level of N^{15} could lie in the region which would greatly affect the rate of energy production in the CN- cycle. At present, the region $O^{16}(He^3, \alpha)O^{15}$ is being studied in this laboratory in an attempt to locate this level in O^{15}.

Method of Extrapolation

A theoretical expression for the reaction cross section (37) is given by

$$\sigma_j(E) = \frac{4\pi k_\ell}{k_j} \sum_J g_J \left| \sum_u^J \frac{\gamma_{uj}\gamma_{u\ell}}{E_u - E - \frac{1}{2} i\Gamma_{uu}} \right|^2 \qquad (4.7)$$

where

j refers to the incident particle, ℓ refers to the reaction product, and u refers to a particular resonance

g_J is the statistical weight factor given by $\frac{2J+1}{(2j+1)(2j'+1)}$

k is the wave number

E is the energy of the incident particle

Γ is the observed width of the resonance, $\Gamma \ll$ level spacing

γ^2 is the reduced width

J is the spin of the state

Within the accuracy of the present experiment, the cross section can be represented by three terms: a term representing the 278 kev resonance, a term for the constant phase s-wave background with J = 1/2 and a term for the constant phase s-wave background with J = 3/2. This representation implies only s-wave contribution to the cross section in the energy range of the experiment. The constant phase background implies that other resonances are distant. Equation 4.7 can then be written as

$$\sigma(E) = \frac{\sqrt{E}\,P_o}{E}\left[\left|\frac{k_1}{E - 278 + 0.85i} + k_2 e^{i\delta_2}\right|^2 + k_3^2\right] \qquad (4.8)$$

where

E is the proton lab energy in kev

P_o is the Coulomb penetration factor for s-wave protons

k_1, k_2, k_3 and δ_2 are experimentally determined constants.

This equation can also be written in the form

$$\frac{E\sigma}{\sqrt{E}P_o} = \left[\frac{k_1^2}{(E-278)^2 + 0.7} + \frac{2k_1k_2 \cos(\delta-\delta_2)}{\sqrt{(E-278)^2 + 0.7}} + k_2^2 + k_3^2 \right] \qquad (4.9)$$

where

$$-\cot\delta = \frac{(E - 278)}{0.85} .$$

Equation 4.9 is convenient to use in evaluating the constants k_1, k_2, k_3 and δ_2. A plot of the function, $(E\sigma)/(\sqrt{E}P_o)$, on logarithmic scale is shown in fig. 19.

It is seen that this function is almost constant above 450 kev. The value of $k_2^2 + k_3^2$ is found to be 6.0×10^{-27} kev-cm^2. The constant, k_1^2, evaluated at the peak of the 278 kev resonance is 2.0×10^{-23} kev-cm^2.

The present experiment is not accurate enough to evaluate the ratio, k_2/k_3, and the constant, δ_2. There is evidence based on very poor cross-section accuracy at 220 kev for a small amount of destructive interference below the 278 kev resonance. The curve for $\delta_2 = 0$ and $k_2/k_3 = 0.4$ is shown in fig. 19.

Since the resonance term and the interference term of equation 4.9 show no appreciable contribution to the measured cross section 150 kev above the resonance, the value of the cross section from 0 to 130 kev can be expressed by

$$\sigma(E) = \frac{\sqrt{E}P_o}{E}(k_2^2 + k_3^2) \qquad (4.10)$$

The value of $k_2^2 + k_3^2$ is constant if there are no resonances near the energy region between 0 and 130 kev.

From the measurements of Duncan and Perry (3), it is seen that most of the s-wave background at 500 kev is due to a level at 9.8 Mev

with a width of 1.2 Mev. Assuming that the 9.8 Mev state is the only source of s-wave background below 130 kev, the value of $k_2^2 + k_3^2$ in equation 4.10 would be approximately 60 °/o of the value determined for $k_2^2 + k_3^2$ at 500 kev. States below 7.347 Mev in O^{15} would cause $k_2^2 + k_3^2$ in the energy region between 0 and 130 kev to be greater than the value determined for $k_2^2 + k_3^2$ at 500 kev.

For computing the rate of energy production in the CN- cycle, it is convenient to write the cross section as

$$\sigma(E_{cm}) = \frac{S_o}{E_{cm}} \exp\left(-\frac{212.3}{E_{cm}}\right) \qquad (4.11)$$

where E_{cm} is the center of mass proton energy in kev. The value of S_o at 25 kev is 2.8×10^{-24} kev-cm^2 for constant $k_2^2 + k_3^2$; S_o is 1.8×10^{-24} for $k_2^2 + k_3^2$ determined by the 9.8 Mev state.

Comparison with Cross Section Measurements Near 130 kev

The reaction cross section has been measured near 130 kev by Woodbury, Hall and Fowler (2) and recently by Lamb (38). The two measurements differ by almost a factor of 10. The Woodbury measurement involved reaction counting rates less than background and it is likely that the error in this experiment is much greater than Lamb's.

The present work when extrapolated to 130 kev is in good agreement with the cross section determined by Lamb. The value, $S_o = 2.8 \times 10^{-24}$ kev-cm^2, is approximately 20 °/o higher than Lamb's value of S_o but is well within the accuracy of the experiments and the extra-

polation (see fig. 19).

Rate of the CN- Cycle

The rate of the CN- cycle is uncertain due to the possibility of a state near 7.4 Mev in O^{15}. The present experiment has shown, on the basis of known levels in N^{15} and O^{15}, that there is one level undetected in O^{15} between 6.26 Mev and 7.6 Mev. The value of S_o determined in Section IV-2 is thus a lower limit for the CN- cycle. An upper limit to S_o is determined by the $C^{12}(p, \gamma)N^{13}$ reaction which is the slowest reaction of the CN- cycle excluding the $N^{14}(p, \gamma)O^{15}$ reaction.

Burbidge, Burbidge, Fowler and Hoyle (39) have computed the rate of energy production in the CN- cycle based on the value of S_o determined in this experiment and also for S_o determined by the $C^{12}(p, \gamma)$ reaction (40). The rate of energy production in the CN- cycle based on the present experiment is a factor of 10 smaller than the previously accepted value based on the measurement of Woodbury, Hall and Fowler (2).

Other experiments are necessary to locate all the levels in O^{15} near 7.4 Mev and thus definitely determine the rate of the CN- cycle.

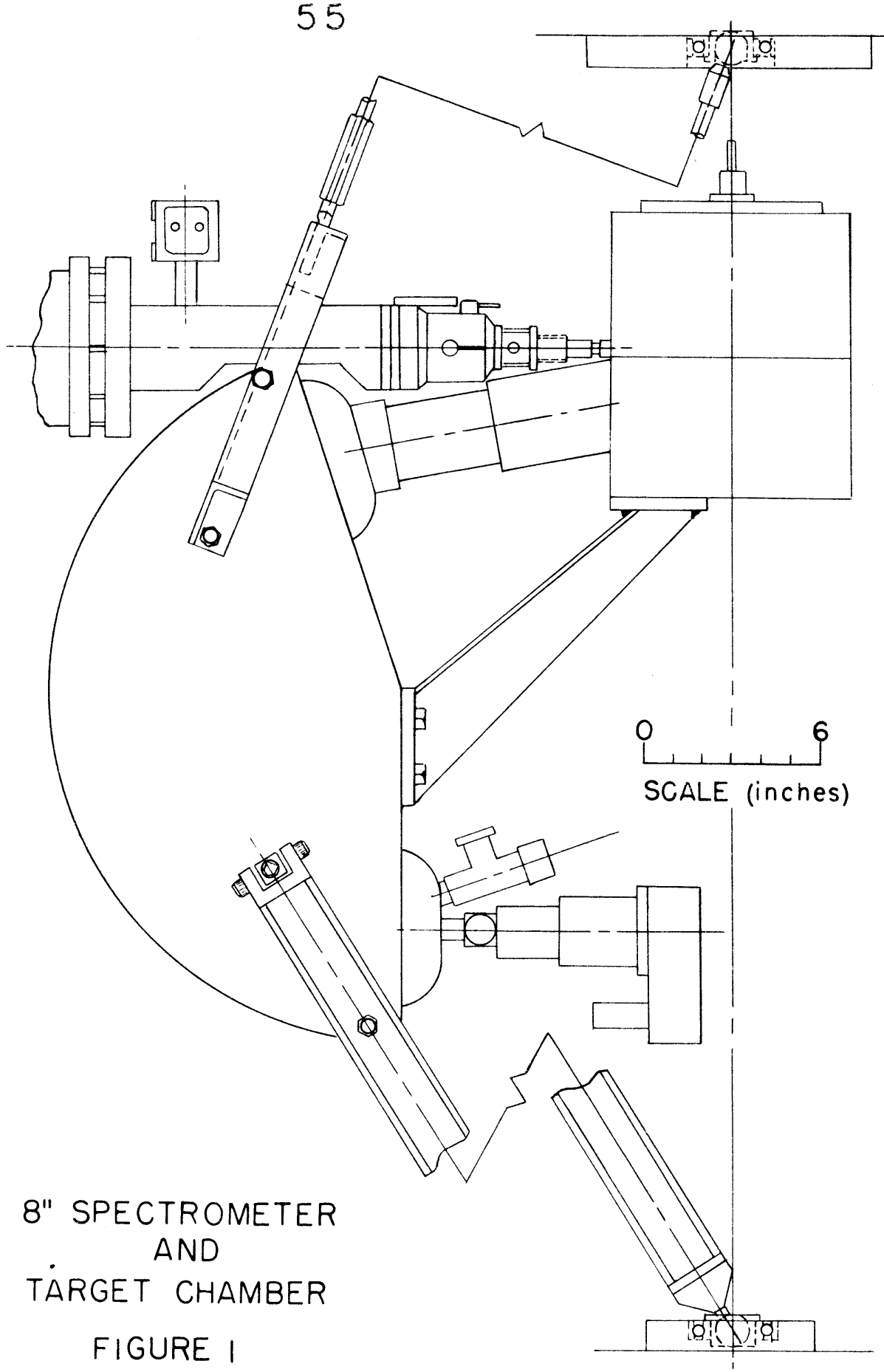

8" SPECTROMETER
AND
TARGET CHAMBER

FIGURE 1

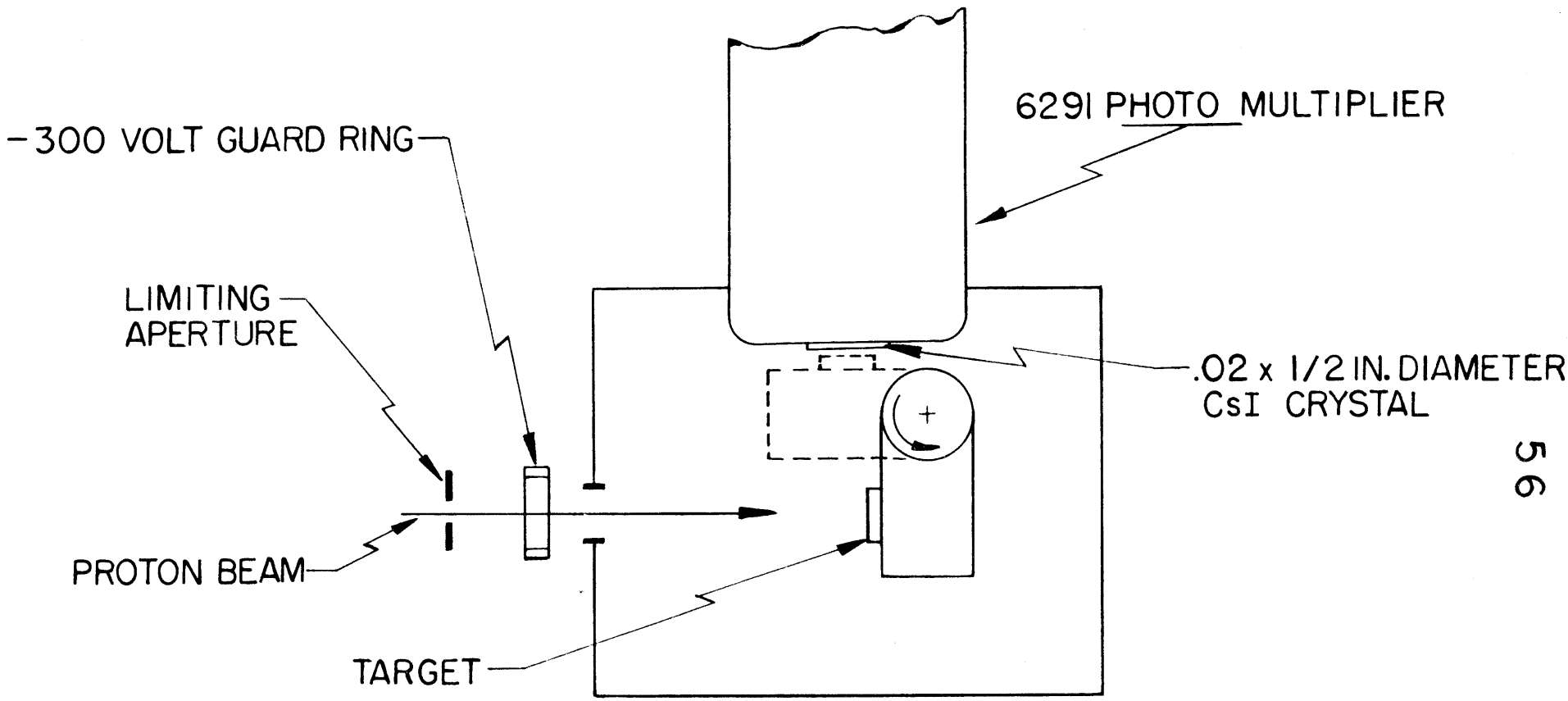

BETA-RAY TARGET CHAMBER

FIGURE 2

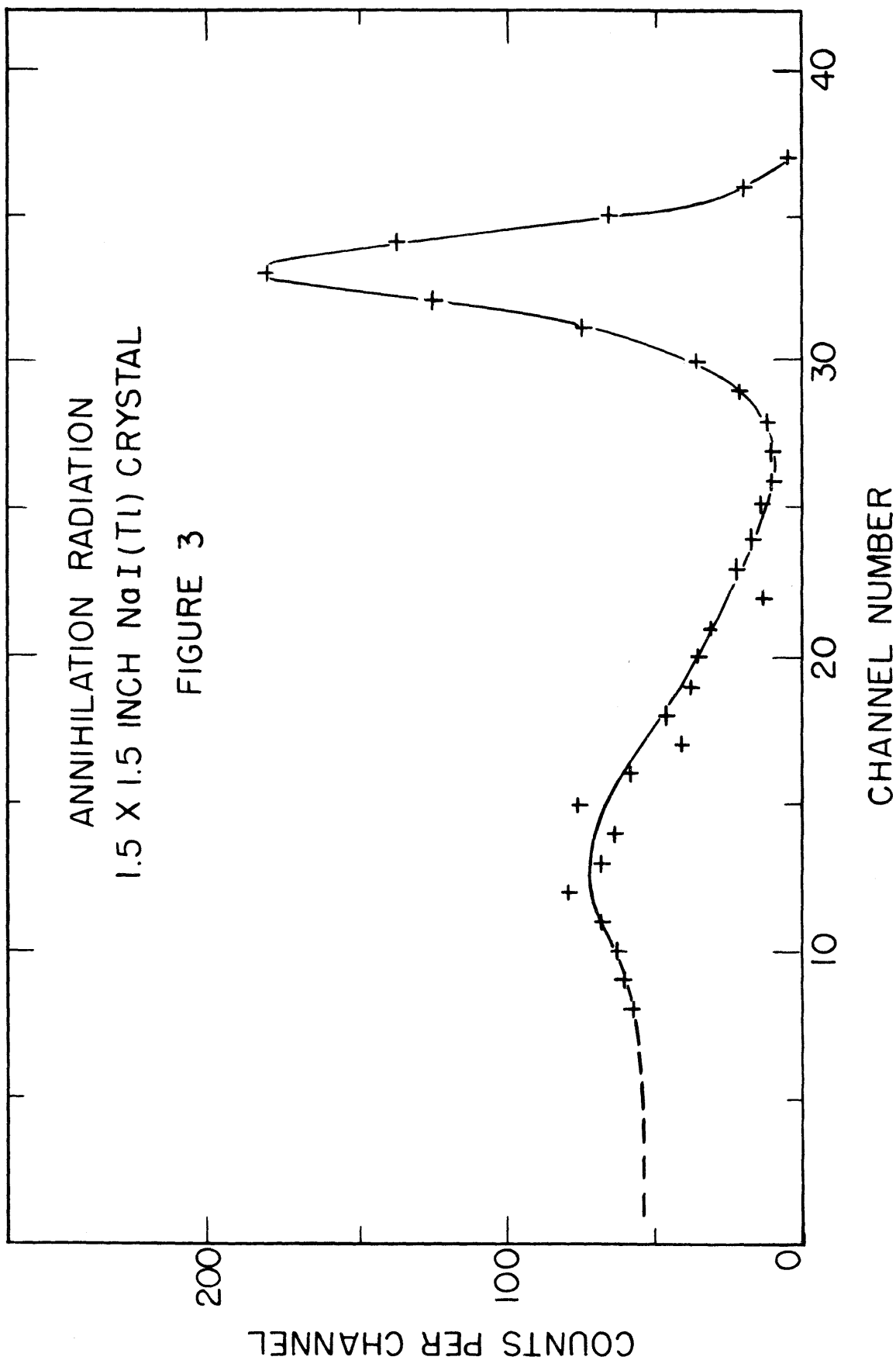
ANNIHILATION RADIATION
1.5 X 1.5 INCH NaI(Tl) CRYSTAL
0
100
200
COUNTS PER CHANNEL
10
20
30
40
CHANNEL NUMBER

FIGURE 3

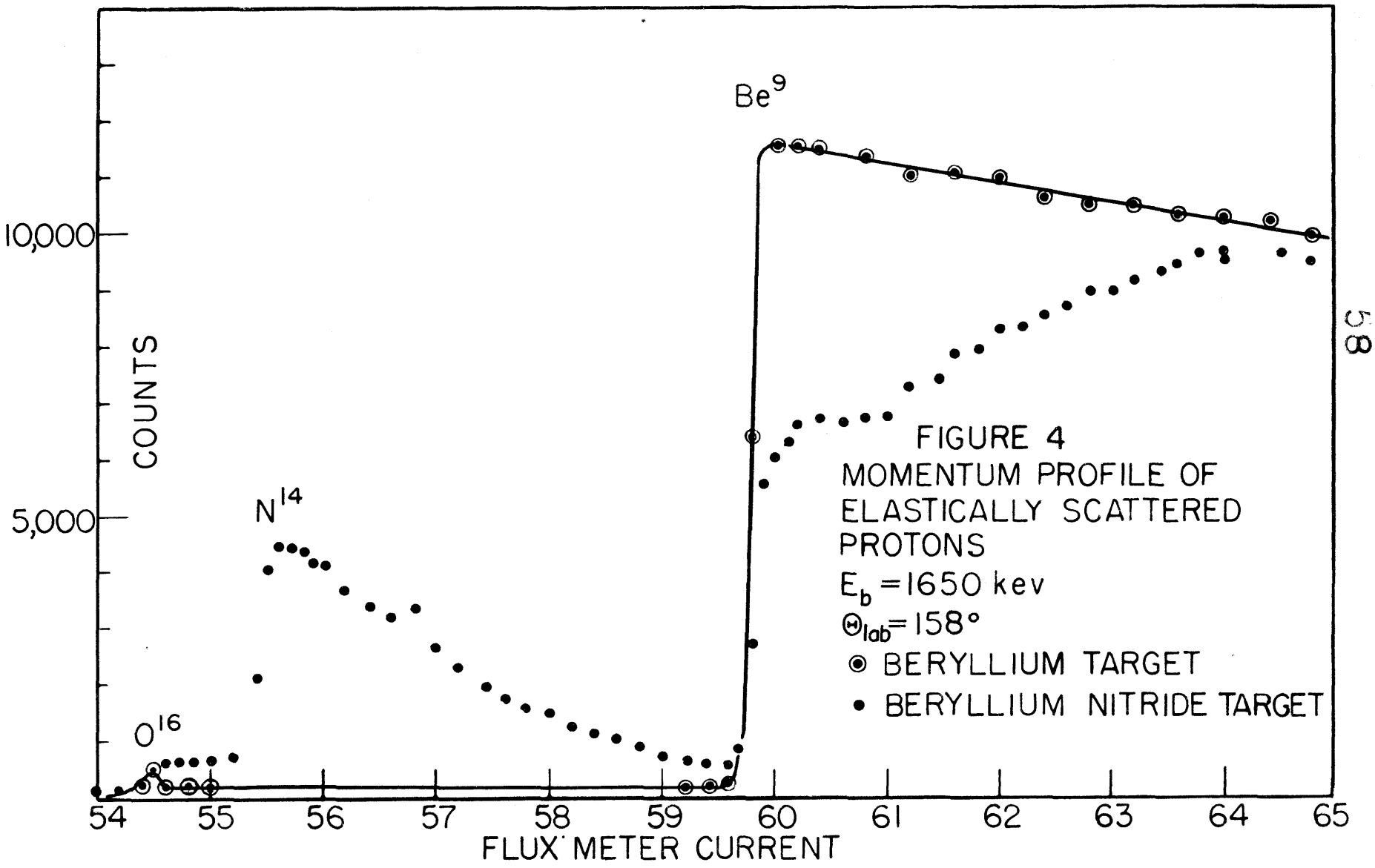
Be9
10,000
5,000
COUNTS
N14
O16
54
55
56
57
58
59
60
61
62
63
64
65
FLUX METER CURRENT
FIGURE 4
MOMENTUM PROFILE OF
ELASTICALLY SCATTERED
PROTONS
Eb = 1650 kev
Θlab = 158°
BERYLLIUM TARGET
BERYLLIUM NITRIDE TARGET

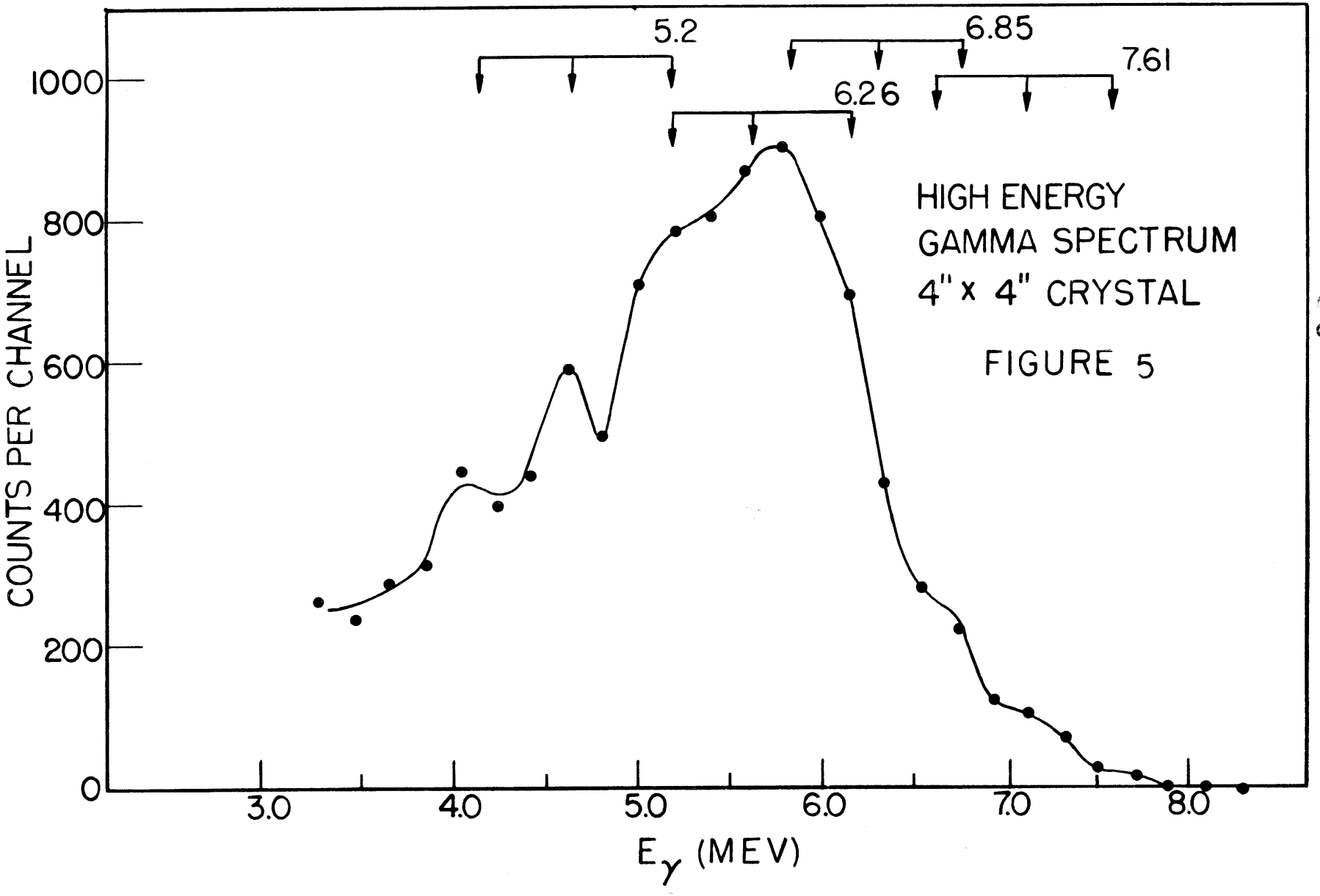
5.2
6.85
7.61
6.26
1000
800
600
400
200
0
COUNTS PER CHANNEL
3.0
4.0
5.0
6.0
7.0
8.0
E_γ (MEV)
HIGH ENERGY
GAMMA SPECTRUM
4" x 4" CRYSTAL

FIGURE 5

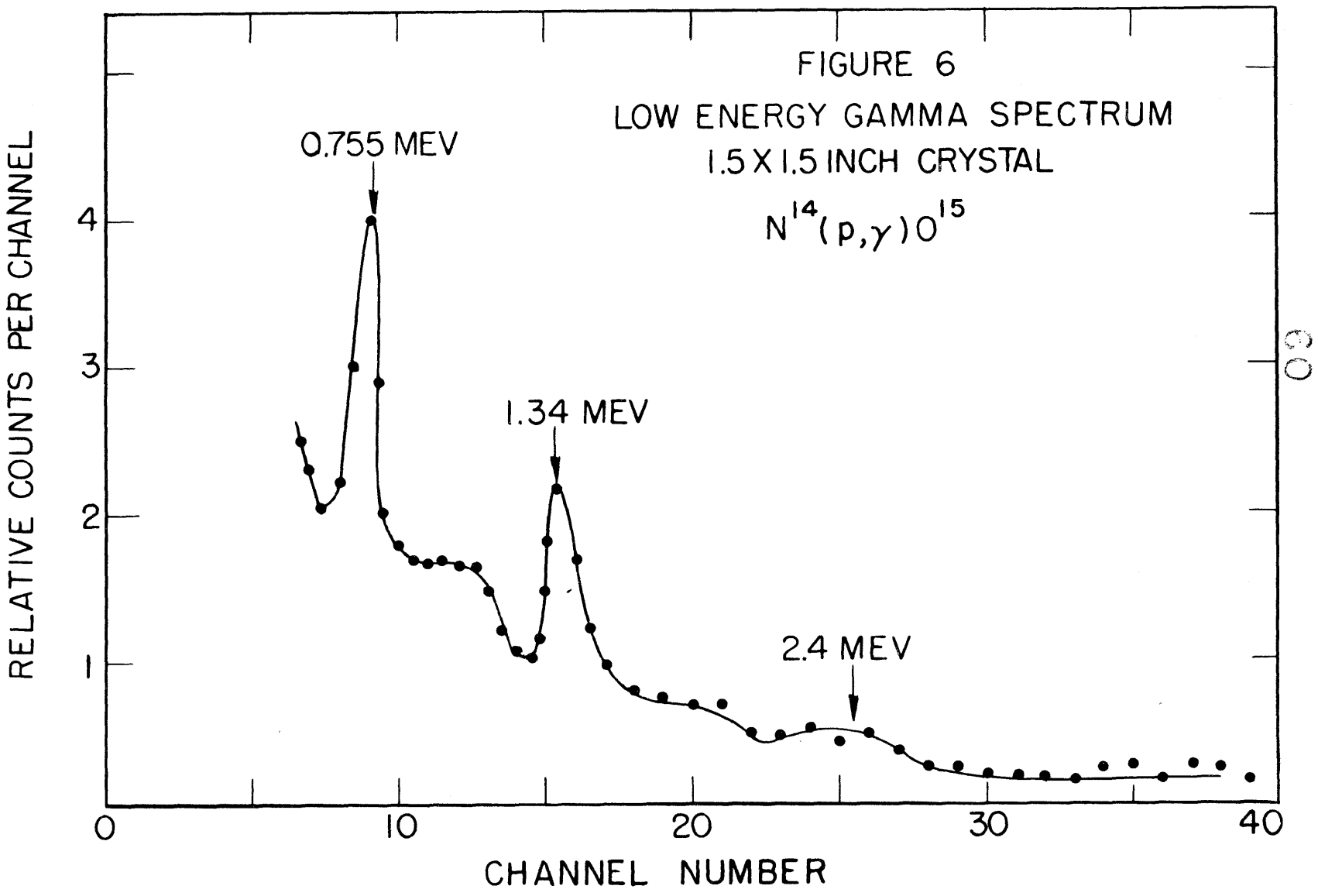
FIGURE 6
LOW ENERGY GAMMA SPECTRUM
1.5 X 1.5 INCH CRYSTAL
$N^{14}(p,\gamma)O^{15}$
0.755 MEV
1.34 MEV
2.4 MEV
RELATIVE COUNTS PER CHANNEL
CHANNEL NUMBER
0
10
20
30
40
1
2
3
4

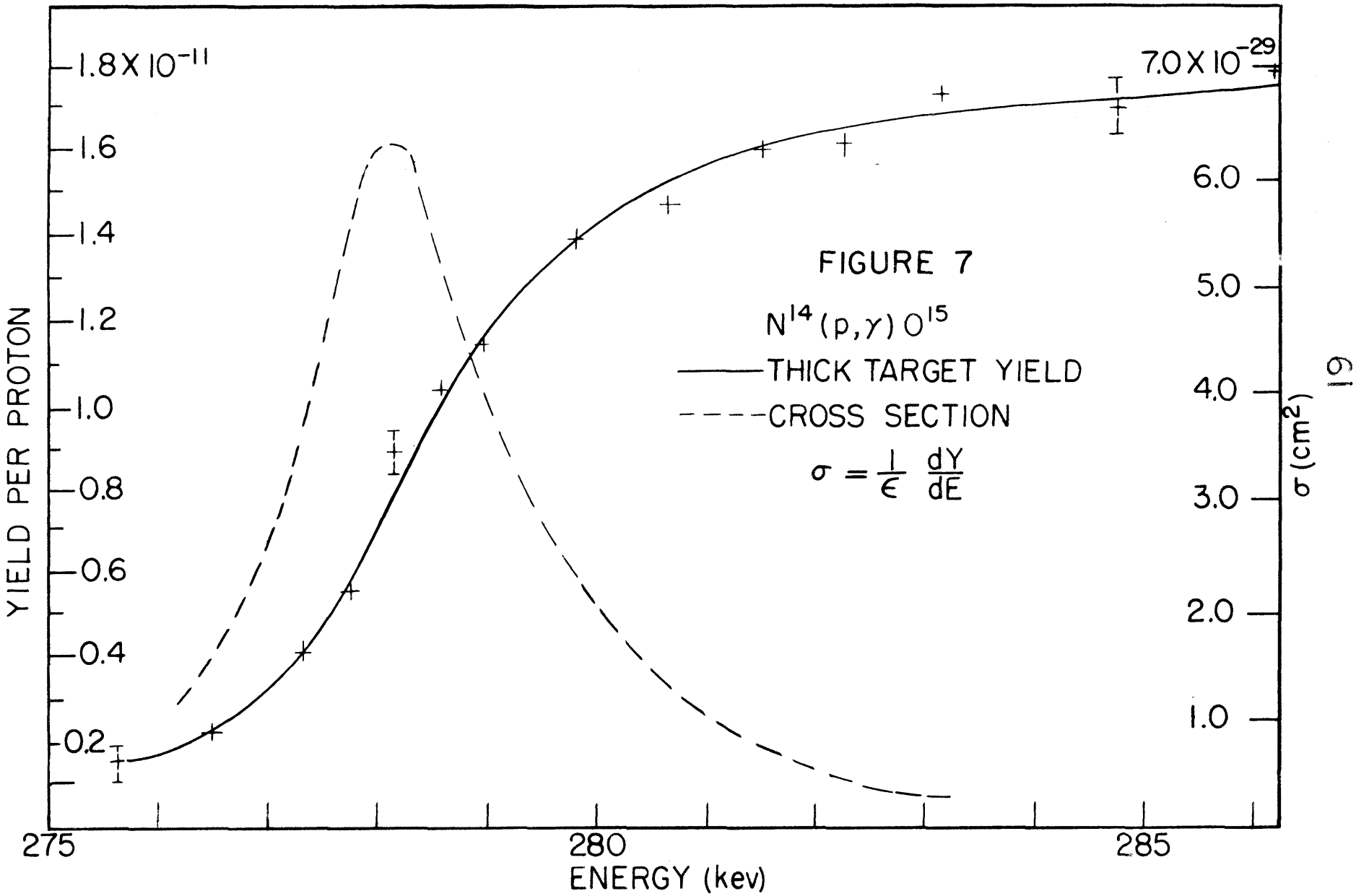
1.8 X 10⁻¹¹
1.6
1.4
1.2
1.0
0.8
0.6
0.4
0.2
YIELD PER PROTON
7.0 X 10⁻²⁹
6.0
5.0
4.0
3.0
2.0
1.0
σ (cm²)
275
280
285
ENERGY (kev)
FIGURE 7
N¹⁴ (p,γ) O¹⁵
THICK TARGET YIELD
CROSS SECTION
σ = 1/ε dY/dE

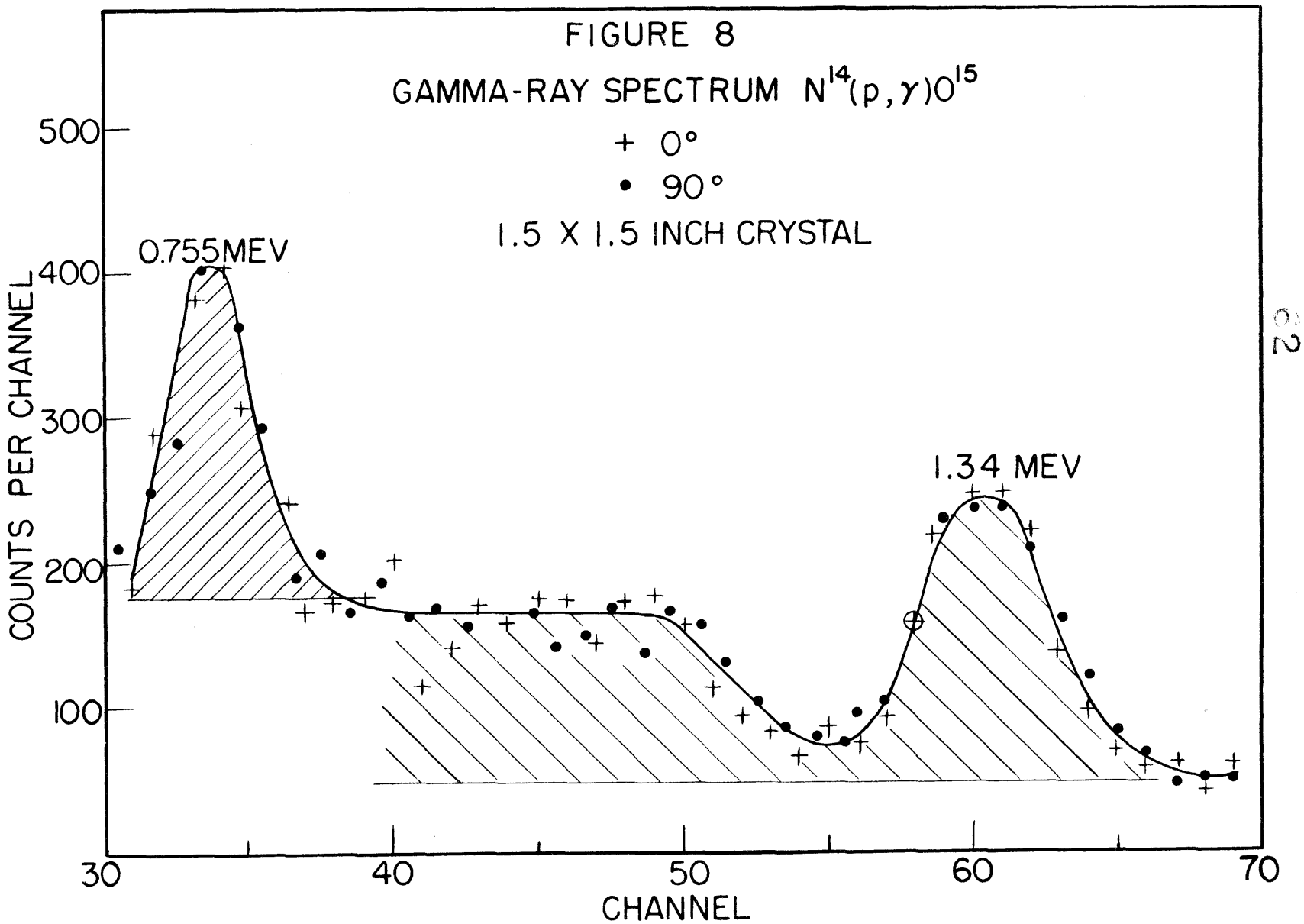
FIGURE 8
GAMMA-RAY SPECTRUM $N^{14}(p,\gamma)O^{15}$
+ 0°
• 90°
1.5 X 1.5 INCH CRYSTAL
0.755MEV
1.34 MEV
COUNTS PER CHANNEL
CHANNEL
500
400
300
200
100
30
40
50
60
70

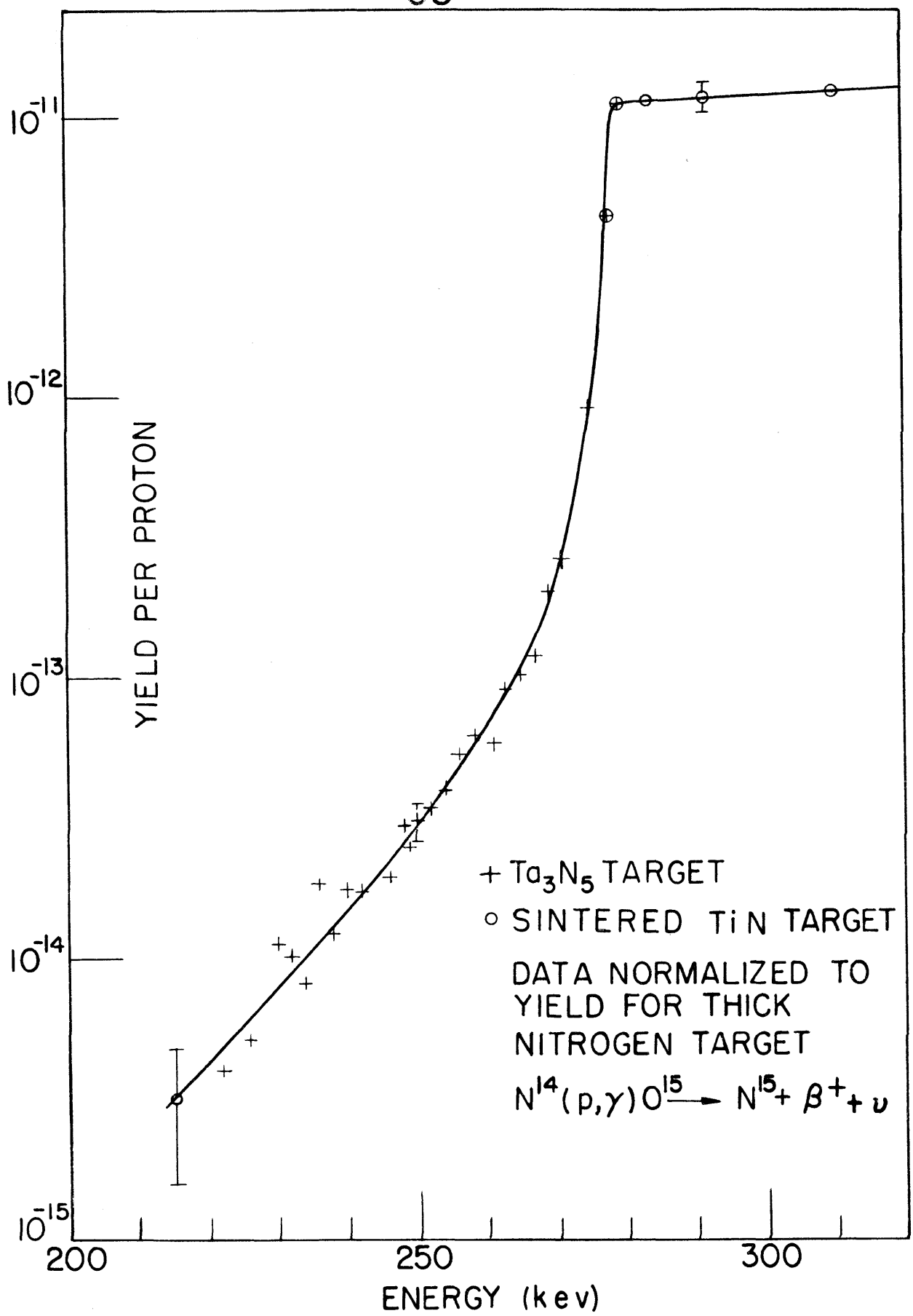
10^{-11}
10^{-12}
10^{-13}
10^{-14}
10^{-15}
YIELD PER PROTON
200
250
300
ENERGY (kev)
+ Ta_3N_5 TARGET
○ SINTERED TiN TARGET
DATA NORMALIZED TO YIELD FOR THICK NITROGEN TARGET
$N^{14}(p,\gamma)O^{15} \rightarrow N^{15} + \beta^+ + \upsilon$

FIGURE 9

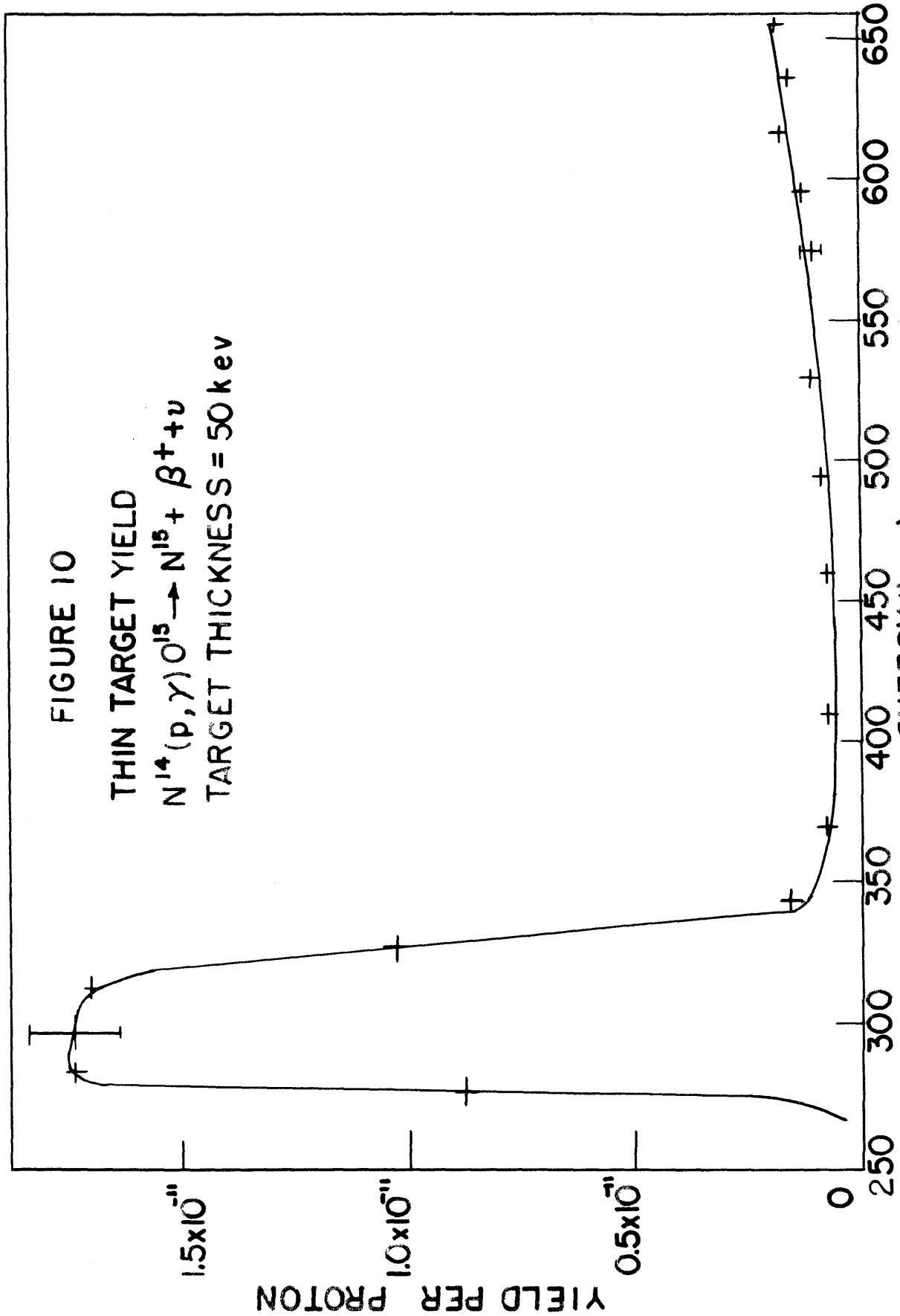
FIGURE 10
THIN TARGET YIELD
$N^{14}(p,\gamma)O^{15} \rightarrow N^{15} + \beta^+ + \upsilon$
TARGET THICKNESS = 50 kev
YIELD PER PROTON
1.5x10⁻¹¹
1.0x10⁻¹¹
0.5x10⁻¹¹
0
250
300
350
400
450
500
550
600
650
ENERGY (kev)

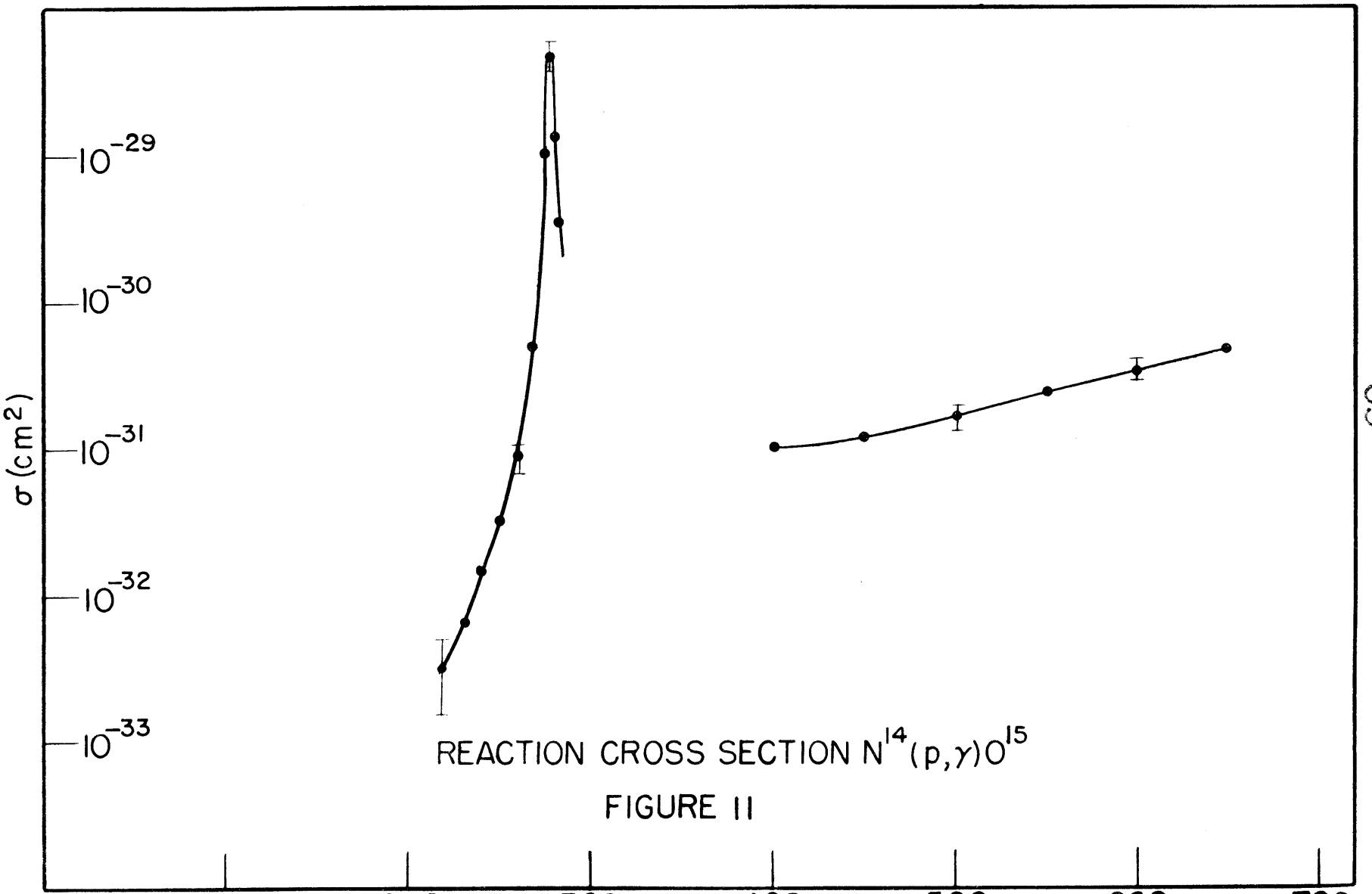

REACTION CROSS SECTION $N^{14}(p,\gamma)O^{15}$

FIGURE 11

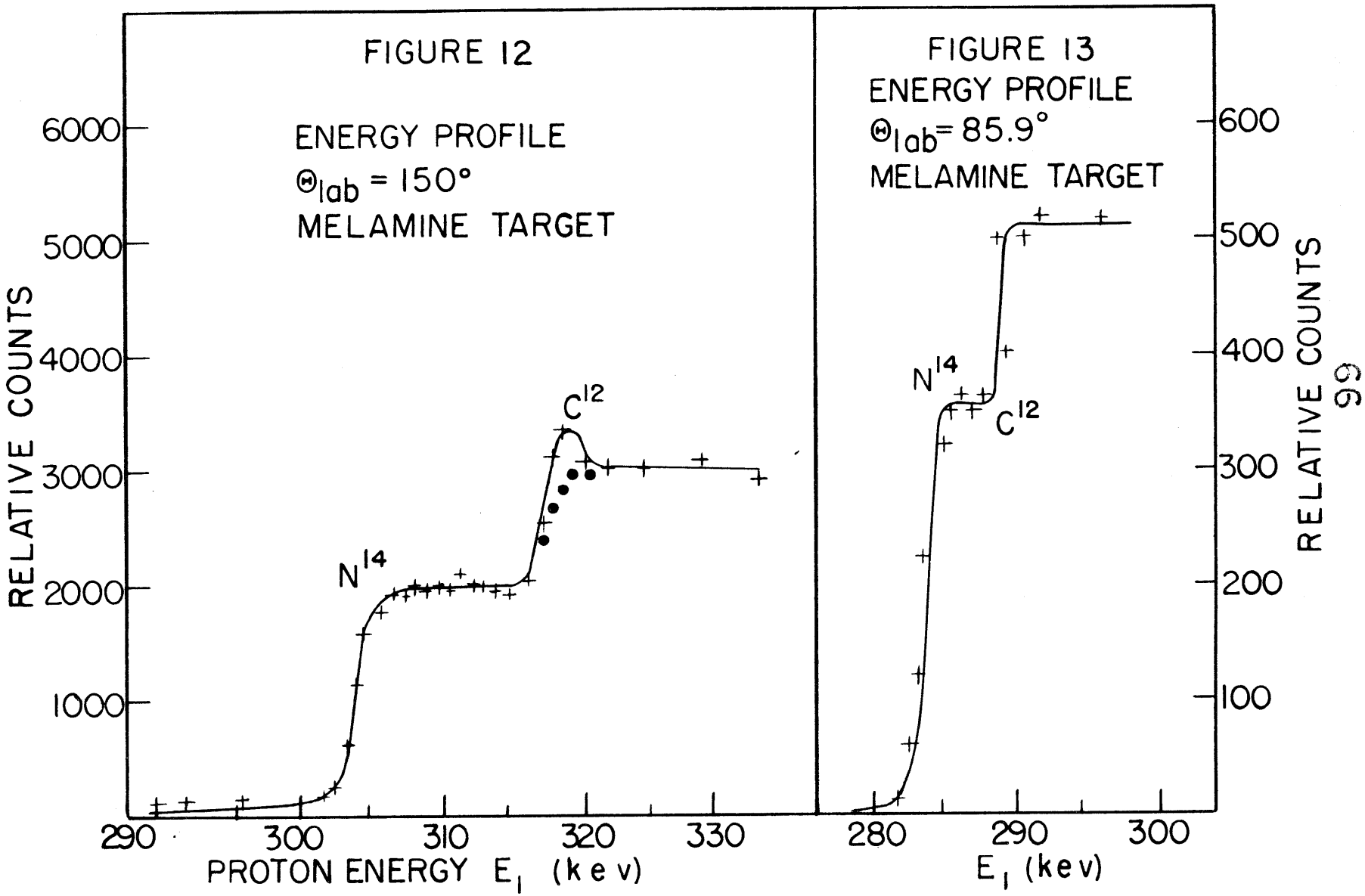
FIGURE 12
ENERGY PROFILE
Θ_{lab} = 150°
MELAMINE TARGET
RELATIVE COUNTS
6000
5000
4000
3000
2000
1000
N^{14}
C^{12}
290
300
310
320
330
PROTON ENERGY E_1 (kev)
FIGURE 13
ENERGY PROFILE
Θ_{lab}= 85.9°
MELAMINE TARGET
600
500
400
300
200
100
N^{14}
C^{12}
280
290
300
E_1 (kev)
RELATIVE COUNTS

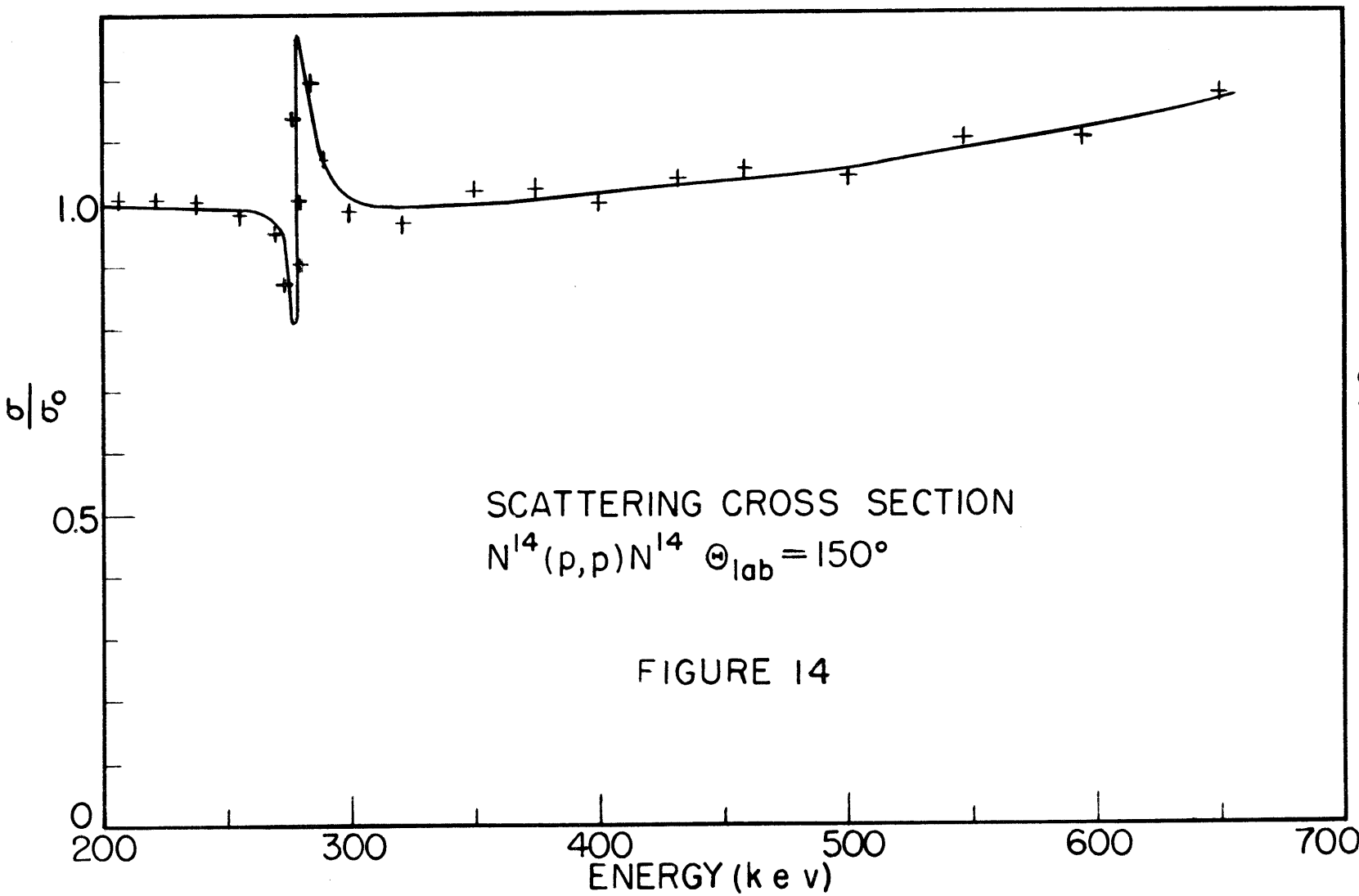
1.0
0.5
0
σ/σ₀
200
300
400
500
600
700
ENERGY (k e v)
SCATTERING CROSS SECTION
N¹⁴(p,p)N¹⁴ Θlab = 150°

FIGURE 14

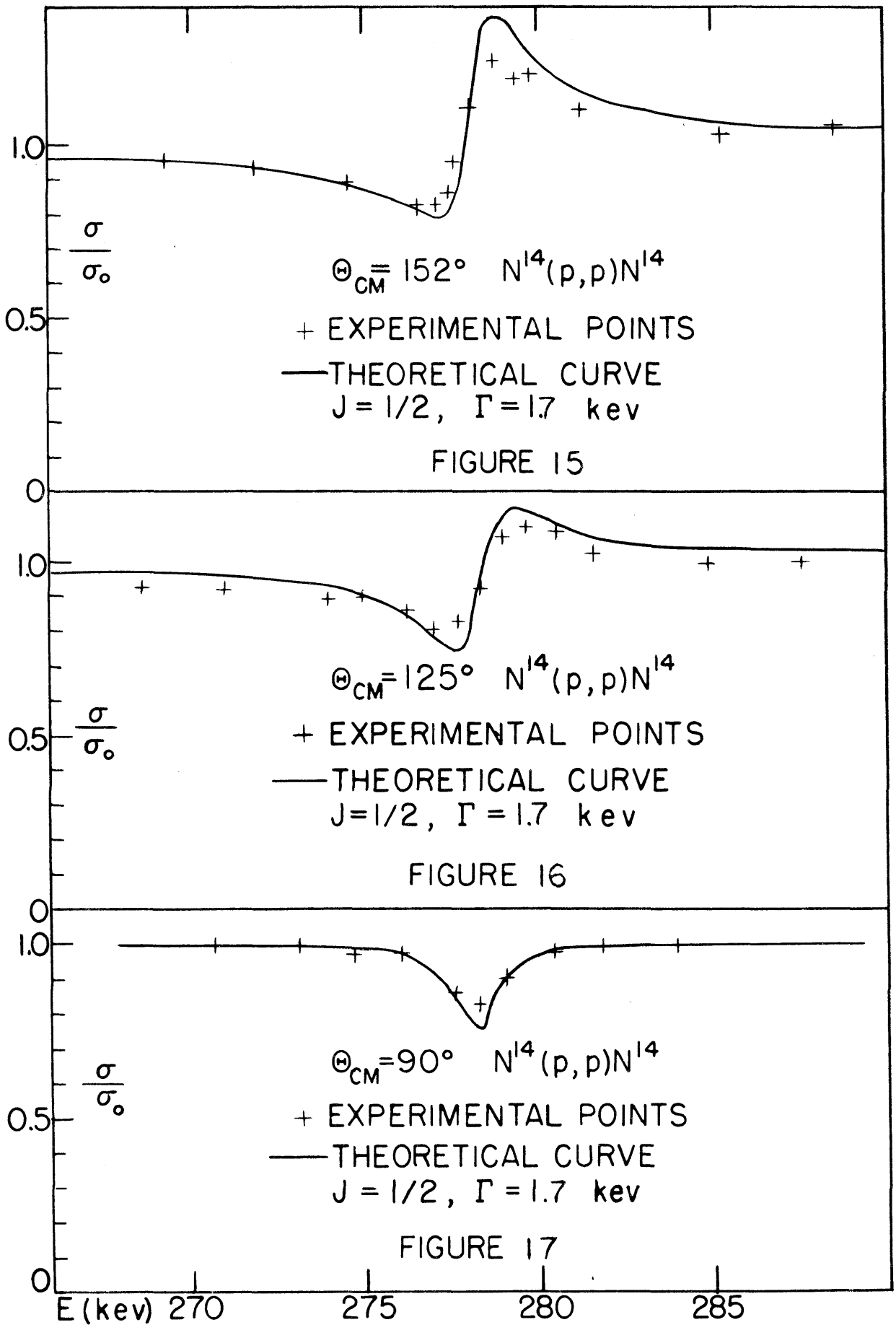

FIGURE 15

FIGURE 16

FIGURE 17

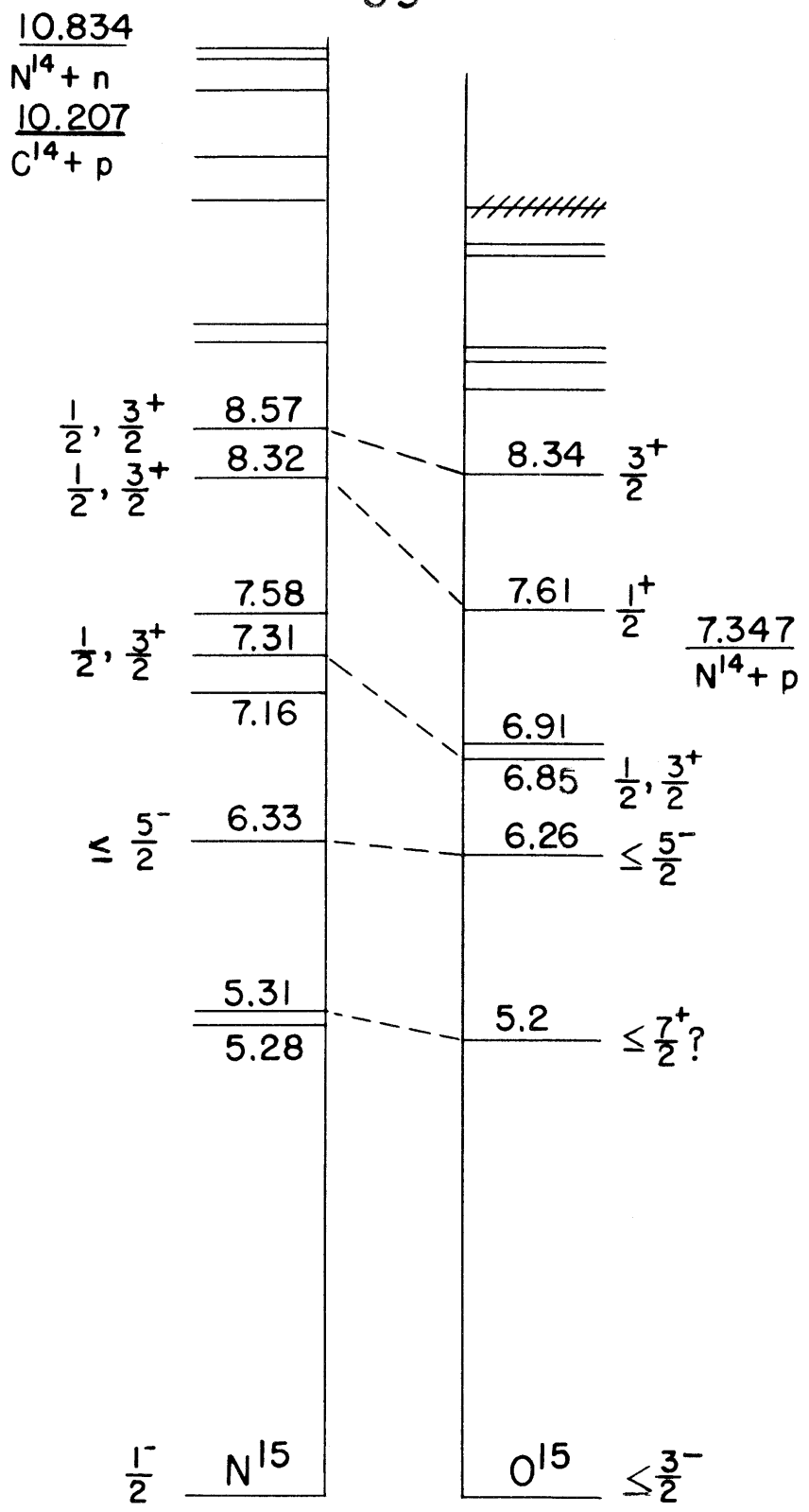

ENERGY LEVELS OF N^{15} AND O^{15}

FIGURE 18

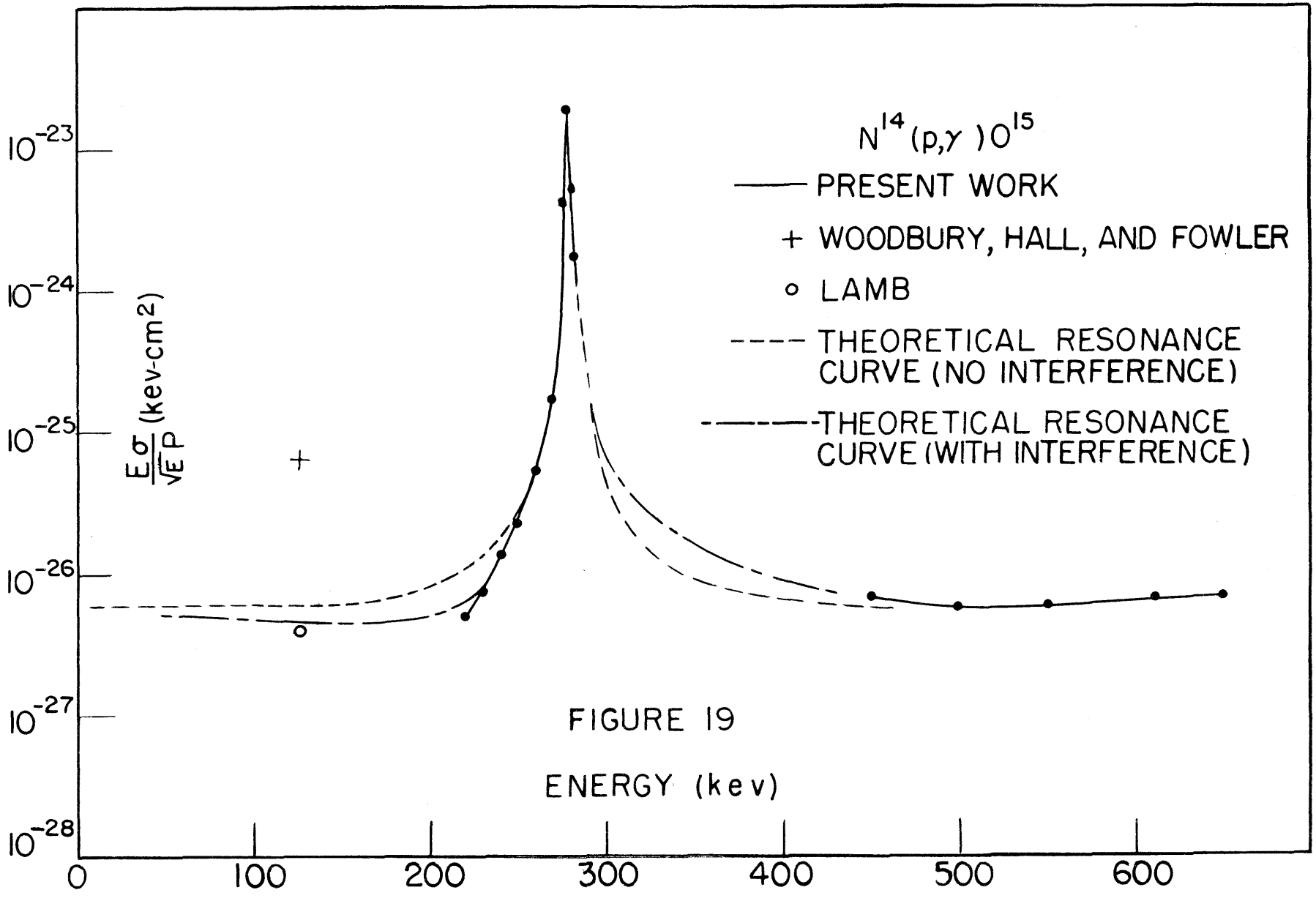
$N^{14}(p,\gamma)O^{15}$
PRESENT WORK
+ WOODBURY, HALL, AND FOWLER
o LAMB
THEORETICAL RESONANCE CURVE (NO INTERFERENCE)
THEORETICAL RESONANCE CURVE (WITH INTERFERENCE)
$\frac{E\sigma}{\sqrt{E}P}$ (kev-cm²)
10^{-23}
10^{-24}
10^{-25}
10^{-26}
10^{-27}
10^{-28}
0
100
200
300
400
500
600
ENERGY (kev)

FIGURE 19

REFERENCES

(1) W. A. Fowler, Memoire Soc. Roy. Sciences de Liege, 14, 88 (1954).

(2) Woodbury, Hall and Fowler, Phys. Rev., 75, 1462 (1949).

(3) D. B. Duncan and J. E. Perry, Phys. Rev., 82, 809 (1951).

(4) Tangen, Kgl. Nord. Vid. Selsk. Skr., N^{o} 1 (1946).

(5) Bashkin, Carlson and Nelson, Phys. Rev., 99, 107 (1955).

(6) W. A. Wenzel, Ph. D. Thesis, California Institute of Technology (1952).

(7) Moak, Reese and Good, Nucleonics, 9, 18 (1951).

(8) Fowler, Lauritsen and Lauritsen, Rev. Sci. Inst., 18, 818 (1947).

(9) Snyder, Rubin, Fowler and Lauritsen, Rev. Sci. Instr., 21, 852 (1950).

(10) P. M. Endt and J. C. Kluyver, Rev. Mod. Phys., 26, 95 (1954).

(11) G. R. White, Natl. Bur. Standards (U. S.) Rept., 1003, (1952).

(12) Kistner, Schwarzschild, Rustad and Alburger, Phys. Rev., 104, 1339 (1957).

(13) Hagedorn, Mozer, Webb, Fowler and Lauritsen, Phys. Rev., 105, 219 (1957).

(14) Laubenstein and Laubenstein, Phys. Rev., 84, 18 (1951).

(15) F. S. Mozer, Phys. Rev., 104, 1386 (1956).

(16) Heydenburg and Temmer, Phys. Rev., 85, 931 (1952).

(17) Herring, Chiba, Gastein and Richards, Bul. Am. Phys. Soc. II, 1, 326 (1956).

(18) J. D. Seagrave, Phys. Rev., 84, 1219 (1951).

(19) Johnson,Robinson and Moak, Phys. Rev., 85, 931 (1952).

(20) S. E. Hunt, Proc. Phys. Soc. (London) A65, 982 (1952).

(21) Fowler, Lauritsen and Lauritsen, Rev. Mod. Phys., 20, 236 (1948).

(22) R. N. Hall, Ph. D. Thesis, California Institute of Technology, (1948).

(23) Ferguson, Clarke, Gove and Sample, Preliminary Report PD-261, Atomic Energy of Canada Limited, Chalk River Project 1956 (unpublished).

(24) Bolmgren, Freier, Likely and Famularo, Phys. Rev., 105, 210 (1957).

(25) Bader, Pixley, Mozer and Whaling, Phys. Rev., 103, 32 (1956).

(26) Wenzel and Whaling, Phys. Rev., 87, 499 (1952).

(27) Reynolds, Dunbar, Wenzel and Whaling, Phys. Rev., 92, 742 (1953).

(28) Allison and Warshaw, Revs. Mod. Phys., 25, 779 (1953).

(29) F. S. Mozer, Ph. D. Thesis, California Institute of Technology (1956).

(30) T. S. Green and R. Middleton, Proc. Phys. Soc. (London) 69A, 28 (1956).

(31) R. D. Sharp and A. Sperduto, MIT Annual Progress Report, 125 (1955).

(32) Evans, Green and Middleton, Proc. Phys. Soc. (London) 66A, 108 (1953).

(33) Marion, Bruggers and Bonner, Phys. Rev., 100, 46 (1955).

(34) R. G. Thomas, Ph. D. Thesis, California Institute of Technology (1951).

(35) Christy and Latter, Revs. Mod. Phys., 20, 185 (1948).

(36) Bloch, Hull, Broyles, Bouricius, Freeman and Breit, Revs. Mod. Phys., 23 (1951).

(37) E. P. Wigner, Phys. Rev., 70, 606 (1946).

(38) W. A. S. Lamb (private communication).

(39) Burbidge, Burbidge, Fowler and Hoyle, Rev. Mod. Phys. (to be published).

(40) R. N. Hall and W. A. Fowler, Phys. Rev., 77, 197 (1950).

APPENDIX

Calculations Involving Nonuniform Targets

The targets used in the yield measurements of this experiment were of nonuniform composition. It is convenient to express the yield obtained from these targets in terms of the yield of a uniform target which has the same composition as the front surface of the nonuniform targets. In order to do this one must know the target composition as a function of depth. An approximate method will be described for determining the composition as a function of depth.

The stopping cross section per nitrogen of a nonuniform target can be written as

$$\epsilon(x, E) = \epsilon_N(E)\left[1 + \sum_{i=1}^{n} \frac{a_i \epsilon_i(E)}{a_N(x)\epsilon_N(E)}\right] = \epsilon_N(E)\left[1 + \frac{A}{a_N(x)}\right] \qquad (5.1)$$

where

$\epsilon_N(E)$ is the stopping cross section of a nitrogen atom

$\epsilon_i(E)$ is the stopping cross section of the i^{th} element

a_N is the number of nitrogen atoms per cm^3 at the depth x

a_i is the number of atoms of the i^{th} element per cm^2

$$A = \sum_{i=1}^{n} \frac{a_i \epsilon_i(E)}{\epsilon_N(E)} \quad .$$

We treat only the case for which the concentration of all elements except nitrogen is constant. The ratio of ϵ_1/ϵ_N does not vary rapidly with energy and is taken to be constant over the energy thickness of the target.

The yield from a target can then be written as

$$Y(E_1) = \int_0^{E_1} \frac{\sigma(E)\, dE}{\epsilon_N(E)\left[1 + \frac{A}{a_N(x)}\right]} \qquad (5.2)$$

where

$Y(E_1)$ is the yield at energy E_1

$\sigma(E)$ is the reaction cross section

x is the depth in the target corresponding to the energy loss $E_1 - E$.

The value of x in equation 5.2 is a function of E_1 and E and thus $a_N(x)$ varies with E over the range of integration.

The value of $\epsilon(0, E_R) / \epsilon(x, E_R)$ can be determined from the measured yield near the 278 kev resonance. The value of $a_N(x)$ and $\epsilon_N(E)$ for the targets used in the present experiment did not vary appreciably over the width of the narrow 278 kev resonance (Γ = 1.7 kev). Equation 5.2 can then be written as

$$Y(E_1) = \frac{\int_0^{E_1} \sigma(E)\, dE}{\epsilon_N(E_R)\left[1 + \frac{A}{a_N(x_R)}\right]} \qquad (5.3)$$

where

E_R is the resonance energy, 278 kev

x_R is the depth corresponding to the energy loss $E_1 - E_R$.

The ratio of the stopping cross sections, $\epsilon(0, E_R) / \epsilon(x, E_R)$, is given by

$$\frac{\epsilon(0, E_R)}{\epsilon(x, E_R)} = \frac{Y(E_1)}{Y(E_R)} \frac{\int_0^{E_R} \sigma(E)\, dE}{\int_0^{E_1} \sigma(E)\, dE} \qquad (5.4)$$

Using the single level resonance form of σ we obtain

$$\frac{\epsilon(0, E_R)}{\epsilon(x, E_R)} = \frac{Y(E_1)}{Y(E_R)} \left[1 + \arctan \frac{E_1 - E_R}{\Gamma/2} \right]^{-1} \qquad (5.5)$$

It is convenient to be able to express x as a simple function of $E_1 - E$. For the targets used in this experiment the nitrogen concentration over the target thickness was represented by a constant and a term linear in x.

$$a_N(x) = a_o + a_o' x \qquad (5.6)$$

Similarly the value of $[\epsilon_N(E)]^{-1}$ over the target energy thickness was represented by a constant and a linear term in $E_1 - E$.

$$\frac{1}{\epsilon_N(E)} = \frac{1}{\epsilon_o} + \frac{1}{\epsilon_o'} (E_1 - E) \qquad (5.7)$$

Using equations 5.1, 5.6 and 5.7 we obtain

$$\Delta E = x(a_o + A)\epsilon_o + \frac{1}{2} \left[\frac{(\Delta E)^2}{\epsilon_o'} + a_o' x^2 \right] \qquad (5.8)$$

where $\Delta E = E_1 - E$. Since the concentration, $a_N(x)$, and the stopping cross section, $\epsilon_N(E)$, vary only a small amount over the thickness of the target, equation 5.8 can be written to first order as

$$\Delta E \cong x(a_o + A)\epsilon_o + \frac{1}{2}\left[\frac{(a_o + A)^2 \epsilon_o^2}{\epsilon_o'} + a_o'\right] x^2 \qquad (5.9)$$

or

$$x \cong \frac{1}{(a_o + A)\epsilon_o}\left\{\Delta E - \frac{1}{2}\left[\frac{1}{\epsilon_o'} + \frac{a_o'}{(a_o + A)^2 \epsilon_o^2}\right](\Delta E)^2\right\} \qquad (5.10)$$

The ratio of nonuniform to uniform target yield, $Y(E_1)/Y_o(E_1)$, at energies below the 278 kev resonance was obtained by using an approximate form of the cross section given in equation 4.9 and the value of $\epsilon(0, E)/\epsilon(x, E)$ as determined above to evaluate the integral in equation 5.2. The approximate form of the cross section is not too critical as the Coulomb penetration factor is changing rapidly with energy and only the cross section near E_1 is important in determining the ratio $Y(E_1)/Y_o(E_1)$.